DAMPING STUDIES IN FLEXURAL VIBRATION

by

Jerome Tomio Uchiyama

A Thesis Submitted to the Faculty of the

DEPARTMENT OF CIVIL ENGINEERING

In Partial Fulfillment of the Requirements
For the Degree of

MASTER OF SCIENCE

In the Graduate College

THE UNIVERSITY OF ARIZONA

1963

STATEMENT BY AUTHOR

This thesis has been submitted in partial fulfillment of requirements for an advanced degree at The University of Arizona and is deposited in The University Library to be made available to borrowers under rules of the Library.

Brief quotations from this thesis are allowable without special permission, provided that accurate acknowledgment of source is made. Requests for permission for extended quotation from or reproduction of the manuscript in whole or in part may be granted by the head of the major department or the Dean of the Graduate College when in their judgment the proposed use of the material is in the interests of scholarship. In all other instances, however, permission must be obtained from the author.

SIGNED: J. T. Uchiyama

APPROVAL BY THESIS DIRECTOR

This thesis has been approved on the date shown below:

Don A. Linger — October 23, 1963

DON A. LINGER
Professor of Civil Engineering

Date

ACKNOWLEDGMENT

The author wishes to acknowledge Dr. D. A. Linger for the many helpful suggestions made during the course of study and the many hours of assistance in the preparation of this manuscript.

TABLE OF CONTENTS

	Page
ABSTRACT	v
Chapter 1 - STATEMENT OF PROBLEM	1
Chapter 2 - GENERAL THEORY	5
Chapter 3 - EXPERIMENTAL PROCEDURE . . .	21
Chapter 4 - DISCUSSION AND CONCLUSIONS .	35
REFERENCES	57
APPENDIX	59

ABSTRACT

An experimental investigation of the dynamic response of bimaterial beams is reported. The effect of adding a viscoelastic material to an elastic material is compared. Two model beams and two prototype beams are studied. Damping forces are evaluated by calculating the response of the system under the action of a constant sinusoidal force and by using logarithmic decrement values of the decay curves.

Results show that the addition of a viscoelastic material to an elastic system does not change the damping mechanism, although a change in the magnitude of damping is noticeable. Experimental results of the prototype beams indicate that the load history of the bimaterial beams strongly affect their response. As a result, interesting nonlinear softening effects and nonlinear damping are encountered in the low stress regions. Suggestions for further studies are presented.

Chapter 1

STATEMENT OF PROBLEM

Introduction

In structural analysis, considerations of the dynamic effects due to earthquake and blast loadings are being given more attention. Standard design codes apply statical amplification factors in structural design where these effects are considered. The application of these dynamic forces result in elastic systems being set into a vibrating motion. This motion is primarily dependent upon the amount of damping in the materials that are used in the geometrical configuration, and upon the interaction of different materials.

When the dynamic forces are removed from the system, the vibrating motion eventually dies out due to internal damping forces. Damping forces in a vibrating system can be derived from a number of sources. In elastic structural systems, the viscous damping is the most familiar and widely used. In viscous damping the damping forces are assumed to be proportional to velocity. In some systems this offers a fair approximation and also yields a simple mathematical solution. However, viscous type damping often does not provide a realistic estimate of the damping characteristic of a structural system. The damping force of structural systems

is often independent of the frequency but strongly effected by the amplitude.

Another linear mathematical theory, in which the damping energy is independent of the frequency, is called the hysteretic damping theory. Hysteretic damping in a single degree of freedom system is similar to the familiar viscous damping in that it implies a resisting force which is in phase with the velocity. Further discussion of this theory is given in the next chapter.

As was stated previously, the amount of damping is dependent upon the type of material and upon the configuration. In addition, two or more materials used simultaneously in a system can take advantage of various types of materials for their energy dissipating characteristics. As a result of this, composite structural systems have been recognized for their ability to dissipate large amounts of energy. It has been found in particular that the addition of viscoelastic materials to an elastic system will greatly increase the magnitude of damping. The addition of a viscoelastic material to an elastic material results in a structural system known as a viscoelastic-elastic bimaterial system.

Objective

The objective of this study was to explore the qualitative aspects of the structural damping of a visco-

elastic-elastic bimaterial system and to attempt to evaluate the primary type and amount of damping in this type of structural system. This study was therefore, and experimental investigation of damping forces in flexural vibrating viscoelastic-elastic systems. The effects of variations in the frequency and amplitude of vibration on the structural systems were studied. The effects on damping properties due to the addition of a viscoelastic element to a vibrating elastic system were also considered. A verification of the composite action between the viscoelastic and elastic material, the type of intermaterial connection, and the amount of increase in damping was attempted.

Scope

Damping forces in a structural system are derived from two major sources; (a) material damping and (b) system damping. This report has not distinguished between these mechanisms of energy dissipation, because the evaluation of the entire system and not the individual components was the objective of this study. The values given therefore are the results of both material and system damping and provide comparative studies for the addition of a viscoelastic material to an elastic system and also for the specific type of connection used between the elastic and viscoelastic materials in the system.

Damping forces can be defined in a number of ways and also, a wide variety of nomenclature is used by different

authors in these definitions. A more complete discussion by several noted authors is given in Reference 12. For this study, the logarithmic decrement and the forced vibration response methods have been used to determine the damping forces. No attempt is made to treat the full dynamical problem, rather, a given simple harmonic motion is used for the beam without reference to the exciting force. Although this approach is grossly simplified, some conclusions can be drawn from the results. The stress level investigated was well within the endurance limit, since the maximum stress did not exceed 3,000 psi in the prototype steel-concrete beam. Only the simply supported configuration was investigated and it is felt that other configurations might be even more informative.

Chapter 2

GENERAL THEORY

History

Investigation of the damping properties of materials was first started in 1784 by Coulomb. He hypothesized and experimentally proved that in torsional oscillation, damping is caused by internal losses in the material. The earliest measurement of internal friction by the free-decay method was performed by W. Weber in 1837. In this method, the logarithmic decrement was observed by watching the rate of decay of the amplitude of vibration. Later investigations were made with models in the form of a wire by T. S. Kê, which proved to be successful.

In 1862, Helmhotz presented a discussion on the steady state bandwidth method as well as the decay-rate method. The bandwidth method denotes a particular analysis in a steady state system. This method, often called the resonant method, employs a harmonic forcing function. The amplitude of vibration is observed as the frequency of the forcing function is varied. The frequency at which the response amplitude is a maximum is called the critical resonant frequency, and width of the amplitude versus forcing frequency curve is a measure of the damping. The resonant

method is employed when the damping forces are large and the response curve is broad. The decay method is somewhat complementary to the resonant method in that if damping is large the resonant method yields good results, but an accurate measurement of the logarithmic decrement is difficult. Conversely, the decay method gives good results when a system is lightly damped, and in which case it is difficult to obtain good results using the resonant method.

In 1912, Hopkinson and Williams presented damping as the hysteretic phenomenon. They suggested that these losses were due to the incongruencies in the stress-strain relationship. This concept was later refined by Föppl when he assumed strain was composed of an elastic and plastic portion, in which the plastic strain causes the hysteresis or energy loss (10)(15).

Theories of Damping

When a mechanical system vibrates, energy is dissipated due to internal damping forces. If the excitation and response are harmonic, or nearly so, the mathematical treatment can fulfil certain ideal conditions. These conditions require that the amplitude of the response, phase angle of the response, and the energy dissipated per cycle should all be related to the frequency and amplitude of the applied forces. For a mathematical solution, it is not required that the magnitude or type of damping be adequately

described or even approximately representative of that in an actual structure. In damping theory, a thorough mathematical treatment is essential. As a consequence, an exact representation of the damping forces is usually sacrificed in order to preserve the linearity of the equations.

The two distinct linear damping theories are the viscous damping theory, and the hysteretic damping theory. A spring with a damper in parallel with the spring can be used to describe the character of the damping theories. If a viscous damper is mounted in parallel with the spring, the damping forces are proportional and in phase with the velocity. For the case of a hysteretic damper, as harmonic motion is initiated into the system, the mechanism of damping has changed. The damping force is proportional to the displacement and in phase with the velocity. An equivalent viscous damping can be used to represent the hysteretic damping in a forced vibration. The results will be the same for both cases for the representation of hysteretic damping if the viscous damping coefficient c is inversely proportional to the forced frequency p.

Viscous Damping The mathematical solution for a viscously damped single degree of freedom system is well established (13). The general linear viscous damping system is often represented as shown in the following figure

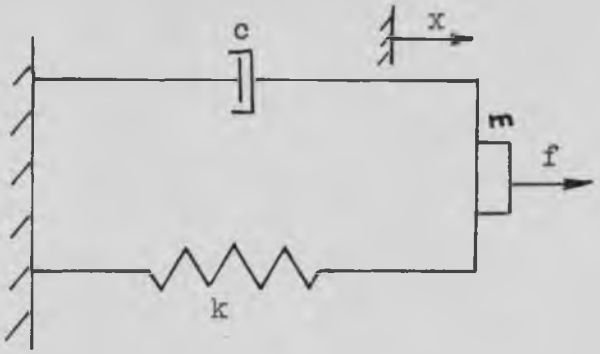

Viscous Damping Model

c = dashpot constant (lb-sec/ft)

k = spring constant (lb/ft)

f = force (lb)

x = displacement (ft)

m = mass (lb-sec^2/ft)

The damping force in viscous damping theory is assumed to be proportional to the velocity. The total force (f) due to an instantaneous displacement (x) is

$$f = kx + c\dot{x}$$

and the equation of motion for a free vibrating system becomes

$$m\ddot{x} + c\dot{x} + kx = 0$$

for which the solution has the form

$$x = e^{-\frac{ct}{2m}}\left[C_1 \cos\left\{\sqrt{\frac{k}{m} - \left(\frac{c}{2m}\right)^2}\right\} t + C_2 \sin\left\{\sqrt{\frac{k}{m} - \left(\frac{c}{2m}\right)^2}\right\} t\right] \quad (1)$$

where

C_1 C_2 = coefficients which depend upon the initial conditions

ω_o = undamped natural circular frequency $\sqrt{k/m}$

ω_d = damped natural circular frequency $= \sqrt{k/m - (c/2m)^2}$

$= \omega_o\sqrt{1 - (c^2/4km)}$; the damping is considered critical when $c = 2\sqrt{km} = c_c$.

For the case of a forced vibration with viscous damping, the equation of motion for a steady-state sinusoidal

forcing function (F sinpt) is

$$m\ddot{x} + c\dot{x} + kx = F \sin pt$$

where p is the forced circular frequency. The solution for this nonhomogeneous differential equation contains two portions; a complementary solution and a particular solution. The complementary part is the free vibration solution given in equation (1). The steady-state portion of the solution of the differential equation is

$$x = A \cos pt + B \sin pt \tag{2}$$

which takes the final form:

$$x = \frac{f}{k} \frac{\sin(pt - \theta)}{\left\{\left[1 - (p/\omega_o)^2\right]^2 + (cp/m\omega_o^2)^2\right\}^{\frac{1}{2}}} \tag{3}$$

where:

$$\theta = \tan^{-1} \frac{-A}{B} = \tan^{-1} \frac{cp}{m(\omega_o^2 - p^2)} .$$

The term

$$\frac{1}{\left\{\left[1 - (p/\omega_o)^2\right]^2 + (cp/m\omega_o^2)^2\right\}^{\frac{1}{2}}} \tag{4}$$

is called the magnification factor. The magnitude of this term is dependent upon the ratio of the forced frequency to the undamped natural frequency and also upon the damping term $(c/m\omega_o)$. When (p/ω_o) approaches unity, the magnification factor is strongly effected by the damping value. A plot of the magnification factor vs (p/ω_o) for different values of $(c/m\omega_o)$ can be found in most vibration texts (13).

To determine the amount of energy dissipated in a viscously damped system, it is assumed that the extension of the spring is given by the displacement function $x = X \sin pt$. The resisting force becomes

$$f = kX \sin pt + cpX \cos pt$$

Eliminating t,

$$f = kx + cp\sqrt{X^2 - x^2}\ .$$

This is an equation of an ellipse which has a major axis which is inclined at $\tan^{-1}k$ to the x-axis

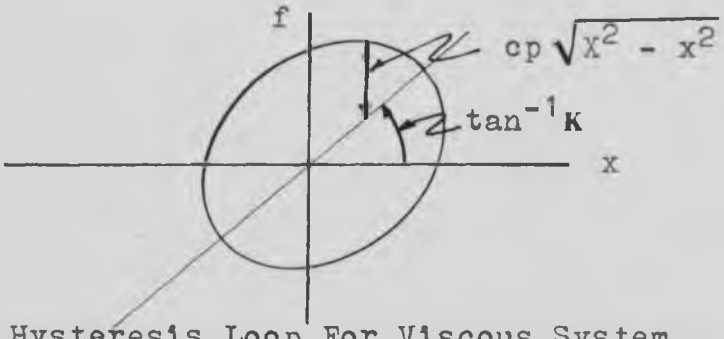

Hysteresis Loop For Viscous System

The area enclosed by the ellipse is

$$E = \oint f\,dx = \int_0^{\frac{2\Pi}{p}} (kX \sin pt + pcX \cos pt)\, pX \cos pt\, dt$$

which reduces to

$$E = X^2 cp\Pi\ . \qquad (5)$$

This is the energy dissipated per cycle by the dashpot. From Equation (5) it is apparent that the energy loss is directly proportional to the frequency and the square of the amplitude.

Hysteretic Damping The term hysteretic damping is derived from a consideration of the energy dissipation in a cyclic deformation of a spring-mass system. The incongruency of the stress-strain relationship or the area enclosed by the loop in a stress-strain diagram represents the mechanical energy dissipated by a material during one complete stress-strain cycle and is therefore an important type of hysteretic damping. Tests have shown that many materials dissipate damping energy in a manner which is independent of the frequency and proportional to the square of the stress amplitude (14). This means that the shape of the hysteresis loop is not changed by the rate-of-strain, and that the stress amplitude changes the size but not the shape of the loop. Moreover, since the energy dissipated in both viscous and hysteretic damping is proportional to the square of the amplitude, a steady-state system with linear hysteresis can be treated as an equivalent viscously damped system with the viscous damping coefficient (c) replaced by the term (h/p). In this equivalent system the hysteretic coefficient (h) depends upon the material and (p) is the frequency of the forcing function. The resulting equation of motion for a single degree of freedom becomes

$$m\ddot{x} + (h/p)\dot{x} + kx = F \cos pt$$

which has a solution of the form

$$x = A \cos(pt - \theta).$$

where $$A = F \frac{1}{\left[(k - mp^2)^2 + h^2\right]^{\frac{1}{2}}}$$

and $$\theta = \tan^{-1} \frac{\mu}{1 - (p/\omega_o)^2} .$$

The energy dissipated per cycle and the form of the hysteresis diagram can be obtained from Equation (5) and the preceeding hysteresis loop for a viscous system by substituting (h/p) for the viscous term (c). The resulting energy dissipated per cycle is

$$E = X^2 h \Pi .$$

For a free vibrating system there are two methods for obtaining a solution. The first method uses a complex representation for the damping force. It is assumed in this approach that for harmonic motion the damping force is proportional to the displacement but in phase with the velocity. The equation of motion becomes

$$m\ddot{x} + k(1 + i\mu)x = 0$$

where $$\mu = h/k .$$

The second method uses an equivalent viscous damping which is applicable when the hysteretic damping is small. The equation of motion for this approach is

$$m\ddot{x} + \frac{h}{\omega}\dot{x} + kx = 0 .$$

The natural damped frequencies derived by the two methods are different. Table 1 shows the relationship between the viscous and the hysteretic damping anaylsis

Table 1
Comparison of viscous and hysteretic damping

	Viscous	Hysteretic	
		equivalent viscous	complex
Force	cx	$(h/p)x$	ihx
Natural frequency	$\sqrt{\frac{k}{m} - \frac{c^2}{4m^2}}$	$\omega_o\left[\frac{\sqrt{1-\mu^2}+1}{2}\right]^{\frac{1}{2}}$	$\omega_o\left[\frac{\sqrt{1+\mu^2}+1}{2}\right]^{\frac{1}{2}}$
Magnification factor	$\frac{1}{\left[\left(1-\frac{p^2}{\omega_o^2}\right)^2+\frac{c^2p^2}{m^2\omega_o^4}\right]^{\frac{1}{2}}}$	$\frac{1}{\left[\left(1-\frac{p^2}{\omega_o^2}\right)^2+\mu^2\right]^{\frac{1}{2}}}$	
Phase angle	$\tan^{-1}\frac{\frac{cp}{m\omega_o^2}}{1-(p/\omega_o)^2}$	$\tan^{-1}\frac{\mu}{1-(p/\omega_o)^2}$	

Damping Energy A common measurement of damping energy dissipated per cycle of vibration is the specific damping energy (D). This measure of damping energy is defined as

$$D = J\sigma^n$$

J = Constant, dependent upon the material and configuration (dimensionless)

σ = stress (psi)

n = damping exponent which relates the amplitude dependency of damping (dimensionless)

For linear damping energy which results from viscous damping,

the specific damping energy (D) increases with the square of the stress. In nonlinear systems the exponent (n) has a value varying from 2 to 3 in the low and intermediate stress regions and a value of 5 to 30 for the high stress regions (8). The specific damping energy is proportional to the area within the stress-strain hysteresis loop. It represents the energy absorbed by a uniformly stressed material. The resulting specific damping energy dissipated per cycle due to the damping forces is equal to $(2\Pi)(\epsilon^2 E_2/2)$. The loss modulus (E_2) is defined as the stress divided by the component of strain that is 90° out of phase with the stress. This form of the specific damping energy (D) is quantitatively applicable only for uniformly stressed specimens. However, since the distribution of stress and the distribution of the stress volume is the same for both model beams and both prototype beams, a qualitative comparison between each type can be made by using the specific damping energy based on maximum fiber stress with no loss of accuracy. Therefore, it was assumed in this study that the specific damping energy for a flexural vibrating beam is equal to the energy dissipated as computed on the basis of the energy loss by the logarithmic decrement and the outer fiber stress. This evaluation of the specific damping energy was done in lieu of an evaluation of the complex stress-volumes in the bimaterial beams.

To evaluate the specific damping in terms of the logarithmic decrement and the stress, it is necessary to define the energy dissipated per cycle in terms of these parameters. The logarithmic decrement (δ), which will be discussed in more detail later, is defined as

$$\frac{X_1}{X_2} = e^{\delta}$$

where X_1 and X_2 are successive amplitudes of vibration. The exponential term can be expanded into a series and by retaining only the first two terms in the series, it can be written as

$$e^{\delta} \approx 1 + \delta$$

This approximation yields

$$\delta = \frac{X_1 - X_2}{X_2} = \frac{\Delta X}{X}$$

The relationship between logarithmic decrement and specific damping energy can be obtained by defining the work energy as

$$W = kX^2$$

The work energy remaining after one cycle is

$$W - \Delta W = k(X - \Delta X)^2$$

where (k) is the spring constant (lb/ft)

(X) is the displacement (ft)

(ΔW) is the work lost per cycle (ft-lb)

The ratio of work energy lost per cycle to the work energy at X becomes, after discarding higher order terms

$$\frac{\Delta W}{W} = \frac{2\Delta X}{X} = 2\delta$$

If the work energy is described by the strain energy, the work lost becomes the specific damping energy. Then

$$\delta \doteq \frac{\Delta W}{2W} = \frac{D}{2(\text{total strain energy})}$$

and by substituting the total strain energy ($\sigma\epsilon/2$) the equation becomes

$$D = \sigma \times \epsilon \times \delta = f(\sigma^2, \delta) \qquad (6)$$

This relationship will be used to correlate the logarithmic decrement values to the specific damping energy values. Using Equation (6), it is seen that if the specific damping energy dissipated for a linear system is proportional to the square of the stress, the logarithmic decrement is independent of the strain. If the logarithmic decrement is a function of the strain amplitude, the the specific damping energy is no longer a function of the square of the strain but of an order higher than two.

Differentiating between a linear and a nonlinear system is done by observing the relationship of the specific damping and strain or stress amplitude ($D = f(\sigma^n)$). If the value of (n) is much greater than 2, the energy dissipated will not be proportional to the square of the stress and the damping system is no longer a linear one. No general solution for arbitrary (n) values have been developed, although there have been empirical relationships suggested. Distinguishing between a linear viscous and a linear hysteresis

damping is accomplished by observing the effects of frequency. The specific damping energy of both types is related to the square of the stress amplitude. For the case of viscous damping the energy dissipated is proportional to the frequency while the hysteretic damping is independent of the frequency. The shape of the loop in the stress-strain diagram is elliptical and its shape is affected by the rate of straining for the viscous condition and the shape remains unchanged for the hysteretic condition.

Another type of damping of interest is a nonlinear form of hysteretic damping which offers a type of analysis where a linear analysis insufficiently describes the problem. The resulting nonlinear system demonstrates a dependence of the motion on the amplitude of vibration for both free and forced vibration systems. From previous investigations, amplitude dependent mechanisms of damping are found to dissipate energy in proportion to the cube of the amplitude in the low and medium stress regions. Values of the 5th to 30th power of the amplitude have been found in the high stress regions (2). Most typical structural systems will be exposed to a wide range of stresses, frequencies and other variables. Damping forces may be dominated by an amplitude dependent or amplitude independent mechanism depending upon the material and stress region. Steel, being elastic is relatively independent of amplitude until the stress approaches the

endurance limit (2).

As the previous discussion indicates, the capacity of a homogeneous material to dissipate energy is often limited to the region of high stresses. Combining two or more materials together offers a method of dissipating larger amounts of energy in both high and low stress regions. Addition of high damping viscoelastic materials to a lightly damped system can increase the damping forces greatly. By proper selection of material and shape, optimization of the damping can be achieved. Addition of a viscoelastic material, which follows closely the linear theory for viscous damping will increase damping but will not change the mechanism of damping in a linear system. In this case the exponent (n) remains constant.

Measurement As a measure of the energy loss per cycle, the logarithmic decrement is used. The logarithmic decrement is obtained from a free vibrating system. A free vibrating single degree of freedom system, which has viscous damping, consists of two factors. The first is a decreasing exponential curve and the second is a sine wave, enveloped by the exponential curve. The term "damped sine wave" is sometimes used to describe this action of viscous damping. During the time interval between two successive maximum peak amplitudes, the amplitude of vibration is diminished

from $X_o e^{-\frac{ct}{2m}}$ to $X_o e^{-\frac{c}{2m}\left(t + \frac{2\Pi}{\omega_d}\right)}$ where (c) is the viscous damping coefficient. The logarithm of the ratios of two consecutive maximums is termed the logarithmic decrement, which for a viscous system is

$$\frac{X_1}{X_2} = e^{\frac{c\Pi}{m\omega_d}}$$

$$\delta = \ln \frac{X_1}{X_2} = \frac{c\Pi}{m\omega_d}$$

A second means of measuring damping forces is by the bandwidth method. The damping is defined by the maximum amplitude response, x_{max}, when a constant force is applied. The frequency at which maximum amplitude occurs is known as resonant frequency (f_o). Points x_1 and x_2, which are equal to .707 x_{max}, are called the half power points. These points are called the half power points because they are the amplitudes at which the power dissipated is one half the power that is dissipated at amplitude x_{max}. The power dissipated due to simple harmonic motion is proportional to the square of the amplitude. Therefore, one half the power at x_{max} will occur with an amplitude of .707 x_{max}, which are known as one half power points. The magnification factor (Table 1) at resonance is

$$M F = \sqrt{\frac{m^2\omega_o^2}{c^2}}$$

This resonance magnification factor, when divided by the square root of two, yields a magnification factor which is applicable to the one half power amplitudes x_1 and x_2. After equating the resulting one half power resonance magnification factor to the general magnification factor term for viscous damping from Table 1 and expanding and solving for $(p/\omega)^2$, the following relationship is obtained:

$$\left(\frac{p}{\omega_o}\right)^2 = 1 - \frac{c^2}{2m^2\omega_o^2} \pm \frac{c}{m\omega}\sqrt{1 + \frac{c^2}{4m^2\omega_o^2}}$$

This can be simplified to obtain the following approximation:

$$\left(\frac{p}{\omega_o}\right)^2 \approx 1 \pm \frac{c}{m\omega_o}$$

Subtracting the two solution of $(p_2/\omega)^2$ and $(p_1/\omega)^2$ yields:

$$\frac{p_2^2 - p_1^2}{\omega_o^2} = \frac{2c}{m\omega_o}$$

Expanding the left hand side of this equation and simplifying results in the following relationship between the forcing frequencies (p_1 and p_2) at one half power amplitudes (x_1 and x_2) and the logarithmic decrement (δ):

$$\frac{p_2 - p_1}{\omega_o} = \frac{c}{m\omega_o} = \frac{\delta}{\Pi}$$

This relationship was used to evaluate the damping for forced vibration conditions. The correlation of damping as determined by logarithmic decrement is presented in Table III.

Chapter 3

EXPERIMENTAL PROCEDURE

Description of Specimens

Two model beams were studied in an initial investigation of the dynamic response of bimaterial beams in flexure. These models were used for preliminary studies of damping forces prior to the testing of larger prototype beams. These models provide an easily controlled method of testing. Both beams were simply supported but were made of different materials. The first model was a 3/4" x 3/8" 2024 clad aluminum bar 50 inches in length. The second model was a 1" x 3/8" cold rolled steel bar 50 inches in length. The viscoelastic material, which was added to the model beams after the first series of tests and prior to the second series of tests, was an epoxy formulation. This changed the elastic system to a viscoelastic-elastic bimaterial system. To insure good bond, the surface was cleaned with methyl ethyl keytone before the epoxy mixture was placed on the beam. These beams are shown in Figure 1. Simple supports for these models were made by inserting tapered tip screws into the sides of the beam at the supports as shown in Figure 1. It is felt that this scheme would allow the least amount of friction during vibration.

The second phase of this experiment was conducted

with two large composite steel-concrete highway bridge beams. The steel beams were 12 inch I beams weighing 50 lb/ft upon which a reinforced concrete slab was connected throughout their lengths of 18 feet 6 inches. Both beams are identical except for the manner in which the concrete was bonded to the steel. One beam was connected by the conventional stud connecters while the other beam was bonded by an epoxy formulation. These beams are shown in Figure 2 and further details can be found in Reference 6. These beams were supplied by the Engineering Research Laboratory at the University of Arizona and had been subjected to dynamic fatigue tests which simulated over a million cycles of live load stress reversal. As a consequence, cracks in the concrete slab were visible which simulated very closely the slab cracking which occurs in many highway bridges. Also, due to the previous cyclic loading, the concrete bond in the stud connected beam had been broken between the top flange and the slab, however, the studs were still intact and functioning as shear connecters.

Instrumentation and Test Equipment

Data was collected on a dual channel Sanborn recorder, model 350-1100B and is shown in Figure 3. This instrument recorded time-strain measurements which provided the information for the determination of the forced response curves and also gave information for the logarithmic

decrement. Bonded SR-4 strain gages were used on all the specimens and were located at midspan on the bottom of the lower flange.

The forcing function necessary to excite the beams was achieved by means of a shaketable. The shaketable is manufactured by the American tool & Mfg. Co., model 10VA. This table has a variable frequency and a variable displacement which provides the necessary control for the forcing function. This is shown in Figure 4.

The large testing apparatus that was used to test the prototype beams is the same test frame that was used to apply the dynamic fatigue loads (6). This is shown in Figure 5.

Test Procedures

Model Beams The forced response method was used as a method of measuring the damping forces. For the two model beams, this was achieved by applying a displacing motion to one support which was secured rigidly to the shaketable while the other support was secured rigidly to a solid foundation. Various prescribed amplitudes were set for the movement of the shaketable which resulted in various amounts of vibration amplitude. The Sanborn recorder was used to record strain versus time by means of the strain gages while the frequency of the shaketable was varied in order to obtain the beam response curves. The arrangement

for this testing of the model beams can be seen in Figure 6. The test was conducted with a constant amplitude setting and by varying the frequency from less than resonance to beyond the resonant frequency. The response of each system was observed throughout the range of the varied frequencies. Several different amplitudes were used for each test beam.

The decay method was used as a second method of measuring damping forces. Each specimen was manually displaced and then suddenly released. The Sanborn instrument recorded strain versus time measurements throughout the decay period. It was observed at certain amplitudes that there were interferences in its first mode of vibration. It was found that by striking the specimen sharply, much of the interference was eliminated. The logarithmic decrement values were computed from measuring successive amplitudes and taking the logarithm of their ratios.

Prototype Beams Damping force measurements for the prototype beams were made in the same manner as those used for the model beams. However, the force response curves were obtained by applying a prescribed forcing function instead of a prescribed displacement, as was done in the model beam test. The physical arrangement for the beams and its supports can be seen in Figures 5, 7, and 8. The shaketable can be seen mounted directly on the center span of the beam in Figure 8. The magnitude of the forcing function was limited by the capacity of the shaketable, however, the

resulting vibratory stresses were still in the range of actual highway bridge live load stresses which were experimentally observed by others (4). The supports for the prototype beams simulated a rocker and roller supporting system which was secured so that no bouncing or adverse movement of the supports occured. Decay curves were obtained by stopping the shaketable and observing the damping. A typical decay curve and also a steady-state response curve is shown in Figure 9.

The model beams have the same basic geometrical shape and also the beams are subjected to the same type of loading. Results will indicate relative differences in their damping character because of these similarities in a model single material to a model bimaterial comparison. The prototype beams are also similar to each other in their shape and loading and comparative results of each other will indicate relative differences in their damping character.

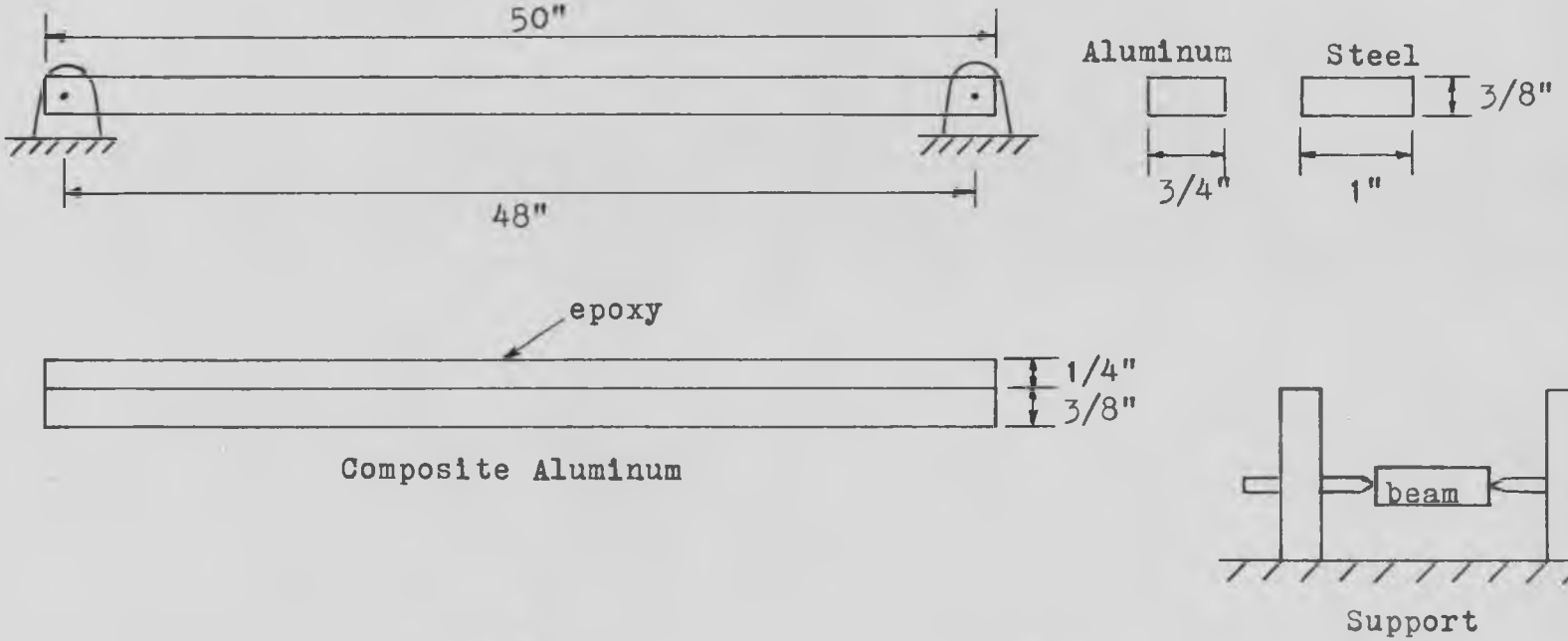

Figure 1

Model Beams

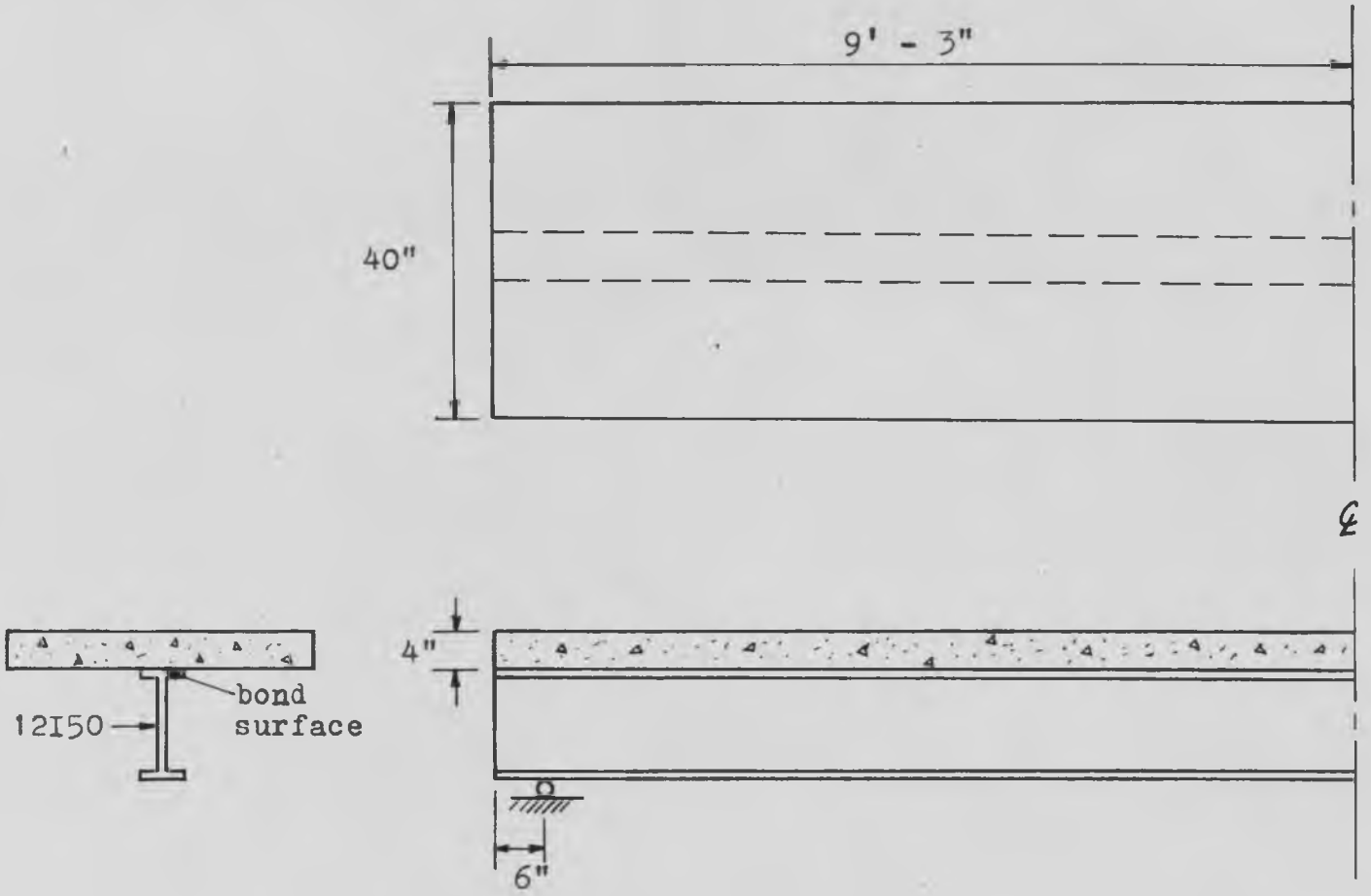

Figure 2

Steel-concrete Prototype Beam

Figure 3
Sanborn Recorder

Figure 4
Variable Shaketable

Figure 5
Prototype Testing Apparatus

Figure 6
Test Arrangement for Model Beams

Figure 7
Support Condition for Prototype Beam

Figure 8
Forcing Function for Prototype Beam

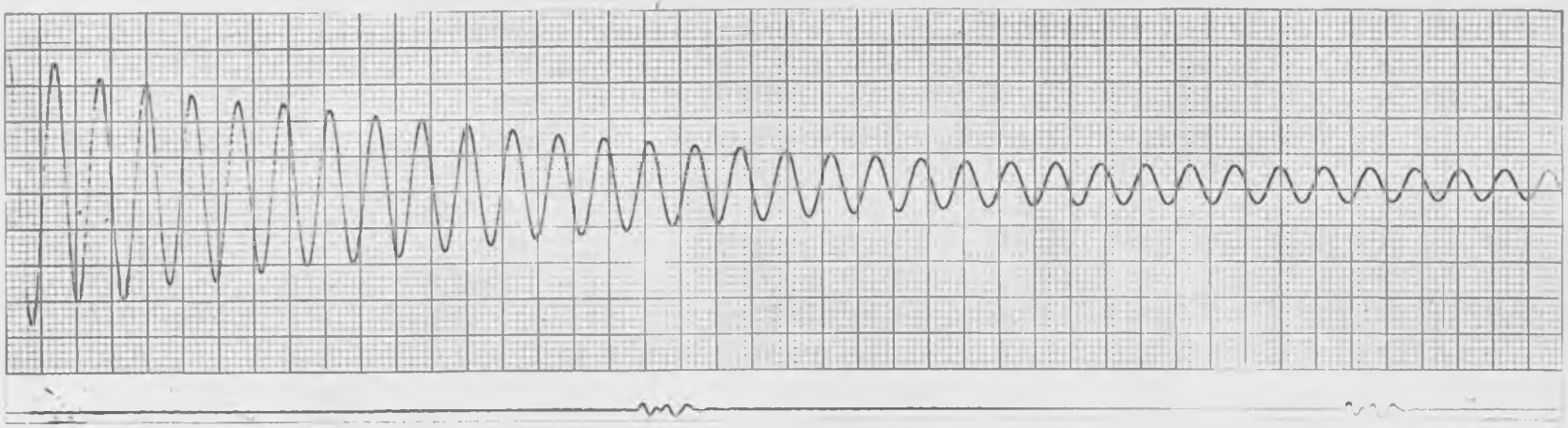

Decay curve for steel model

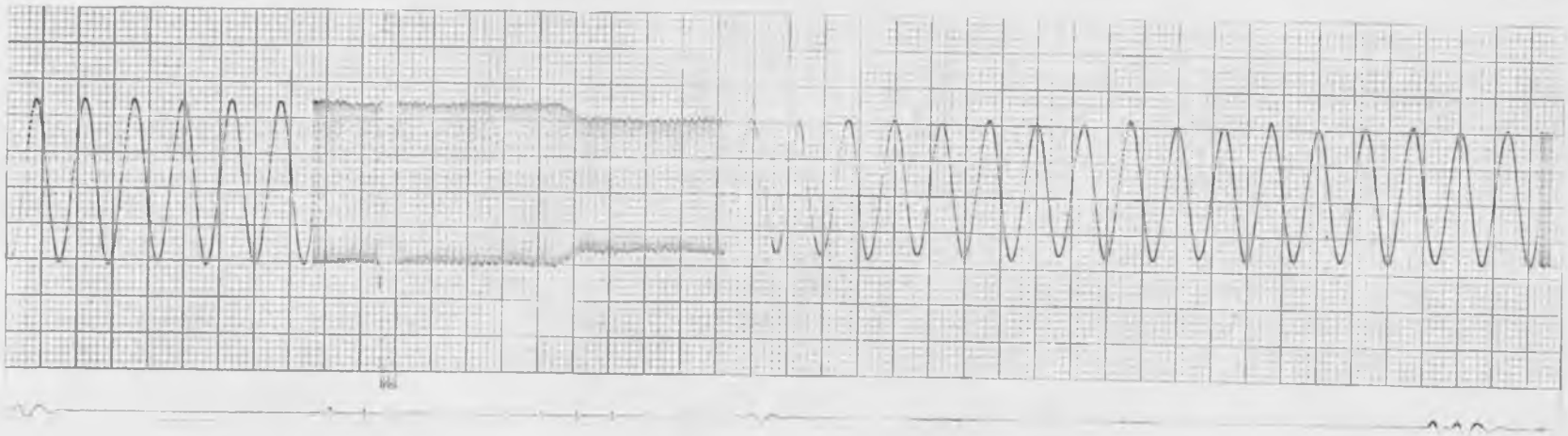

Steady state response

Figure 9

Chapter 4

DISCUSSION AND CONCLUSIONS

Discussion of Results

The studies conducted on the model steel and aluminum beams indicate that a definite increase in the damping forces is developed with the addition of the viscoelastic epoxy material. Figures 10 and 13 show a definite increase in the logarithmic decrement at any particular strain amplitude with the added viscoelastic material. The slope has remained approximately the same which indicate that the mechanisms of damping are similar in their energy absorbing characteristics. The amount of shift of the curves indicates the amount of increased damping. The forced vibration response curves for these beams indicates the change in response which is dependent upon the relative amount of viscoelastic material added to the elastic beam and the ratio of the dynamic elastic moduli of the two materials. This can be noticed by the magnitudes of the change in the natural frequency for resonant condition shown in Figures 11 and 14. Each different curve in these forced response figures and in Figures 17 and 18 represents the response resulting from one magnitude of forcing function. After the magnitude of the forcing function was increased a new response curve was obtained. The resulting family of curves

indicates the amount of damping at each maximum strain amplitude level, and provides an insight into the nonlinearities in the systems. The relationship between the specific damping energy and the stress amplitude, $D=f(^{n})$, as shown in Figures 12 and 15, indicates that (n) is very close to 3.0 and 2.3 for the aluminum and steel model beams respectively. The actual experimental values are given in Table IV. The steel model beam shows a very small increase in the damping with the addition of the epoxy and thus, a much larger amount of secondary material must be added in order to increase the damping in flexure. However, the aluminum beam showed an increase of 50 to 150 percent in its specific damping energy which indicates the strong influence the epoxy had on the damping. Both specimens had nearly the same thickness of epoxy added but the eff of the added epoxy on the stiffness was hardly noticed in the model steel beam. This action can be clearly seen in Figures 11 and 14 by the change in the resonant frequencies due to the added material. The model beams, also, demonstrate a slight nonlinearity by the form of their resonance curves, as shown in Figures 11 and 14. This nonlinearity can be explained by the fact that at higher strain values the damping has increased as is shown in Figures 10 and 13, and as is shown in Table I, the damped natural frequency decreases as the damping increases. The shift in the forced vibration response curves after the addition of epoxy to both model specimens indicates that the

added epoxy layer resulted in a decrease in the natural frequency of the beams. This is the result of the mass of the beam being increased by the epoxy without a proportional increase in the moment of inertia. The ratio of the elastic moduli of the aluminum and steel beams to the epoxy is approximately 152 and 430 respectively.

The results of the prototype beam tests indicates a definite nonlinear character, as shown in Figures 17 and 18, in which the peaks of the resonant response curves shift strongly to the left as the vibrating force increases. Moreover, the experimental response curves of the two beams indicate a resonant frequency in the range of 16 to 20 cps, depending upon the amplitude of the forcing function. From a theoretical calculation, which included the composite action of the concrete, the natural frequency for the first mode of vibration should be 26.8 cps. However, the steel beam alone, with the concrete acting only as a uniform mass, has a theoretical natural frequency for its first mode of vibration as a pinned-pinned beam of 16.1 cps which agrees well with the experimental values obtained. As was indicated in the specimen description, these composite beams had previously been subjected to cyclic loading, therefore, these beams are the equivalent of actual beams which have been in service for a long period of time. As a result of the previous history of the beams, cracking had developed

in the concrete slab, and therefore, during the experimental studies, the beams responded as though the concrete was not acting in a fully composite action with the steel portion of the beam. It is felt that the major factor involved in obtaining the low natural frequencies, was the cracks in the concrete. This would have a tendency to decrease the stiffness of the beam under vibratory loading, although the results from the static load-deflection curve (Figures 20 and 21) indicate a linear composite system. The nonlinearity of the forced response results might also be explained by the decrease in the stiffness resulting from the vibratory action of the concrete. More specifically, the cracks in the slabs were located in the maximum moment region and therefore, it is assumed that the strains induced due to bending were taken up by these cracks. This caused the steel beam to act independently of the concrete slab. However, at the low stress values, the constraining variables which were not yet overcome by the vibration had contributing roles which caused the initial higher resonant frequencies. As these variables were overcome, the beam began to act more independently of the concrete. The initial support friction and the slippage friction in the stud connected beam are thought to be major contributing factors in the initial softening effect. No further investigation was performed on this phase although further studies in this area would be desireable. It appears that the prototype beams

are not truly composite but only partly composite and at some values noncomposite.

Comparing the two prototype beams, the studded beam showed a much greater damping, as shown in Figure 16. It was observed by another investigator (3), who investigated a composite steel-concrete bridge, that slippage between the steel and concrete was one of the main factors involved in contributing to high damping forces. This type of slippage probably occurred in the stud beam as a result of the extensive past loading history of the beam and the possibility of considerable microcracking between the two materials, some of which could be seen. The epoxy bonded beam, on the other hand, had lesser movement between the two materials due to the apparently sound bonding by the epoxy. The experiment performed in this study indicates that the damping due to slippage is more predominate than that due to the stiffness of the material or the structural system, for the amplitudes studied.

The experimental results shown in Figure 19 indicate that the specific damping energy is approximately a function of the square of the stress amplitude. This is indicated by the slope of the curves in Figure 19, which 2.0 and 2.5 for the stud and epoxy bonded beams respectively. The slope of the curves as determined on the log-log plot of Figure 19 is the exponent (n) relating the stress to the specific damping energy. Therefore, an analysis using an equivalent viscous

damping would give good results for the low stress range.

The supporting conditions, which were assumed to be simple supports, were not meticulously investigated. It is felt the contribution of support damping to the damping of the systems was very minor due to the small rotations and restrictions of the ends of the beams, for the low stress region investigated.

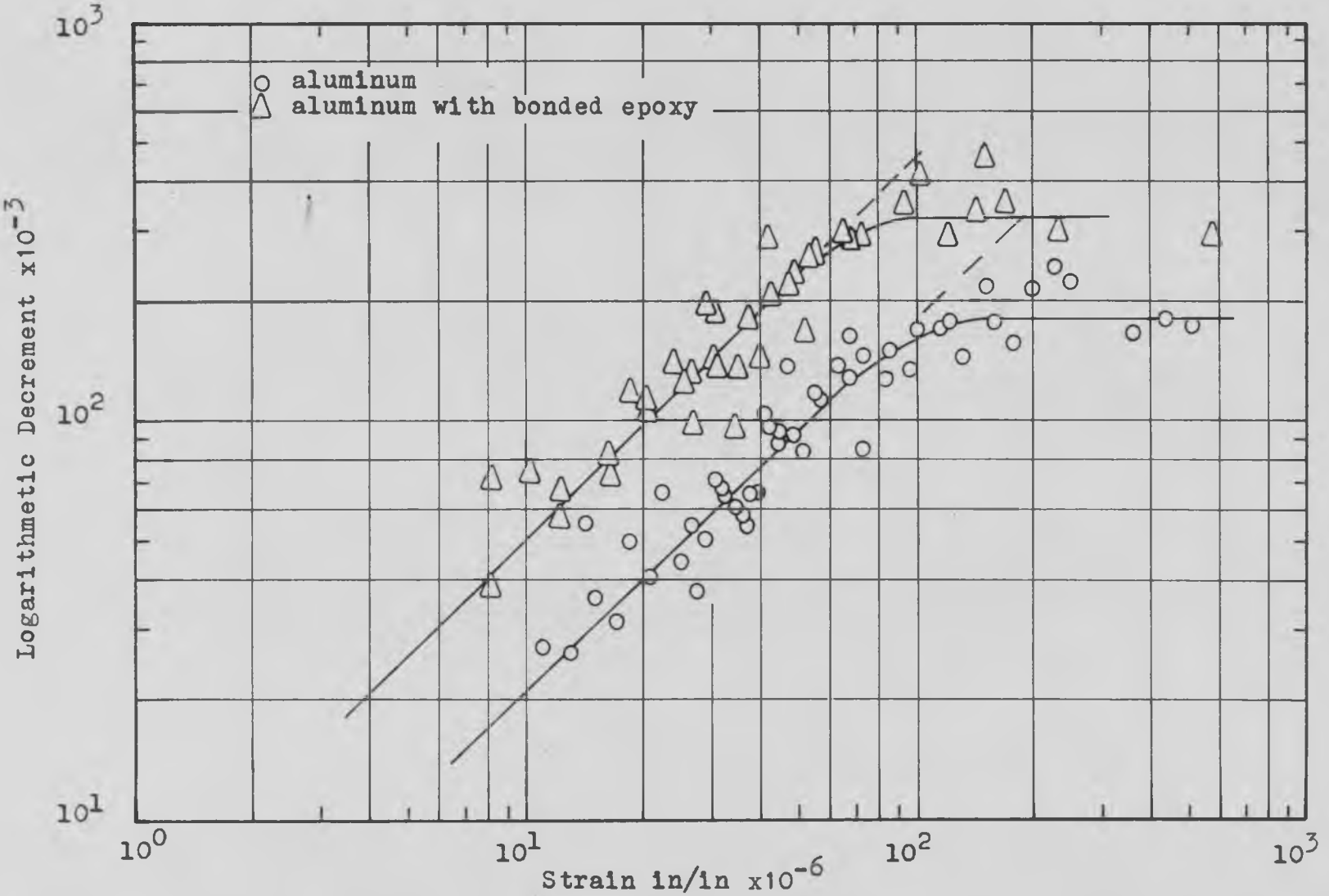

Figure 10
Logarithmic decrement vs strain plot for the model aluminum beam

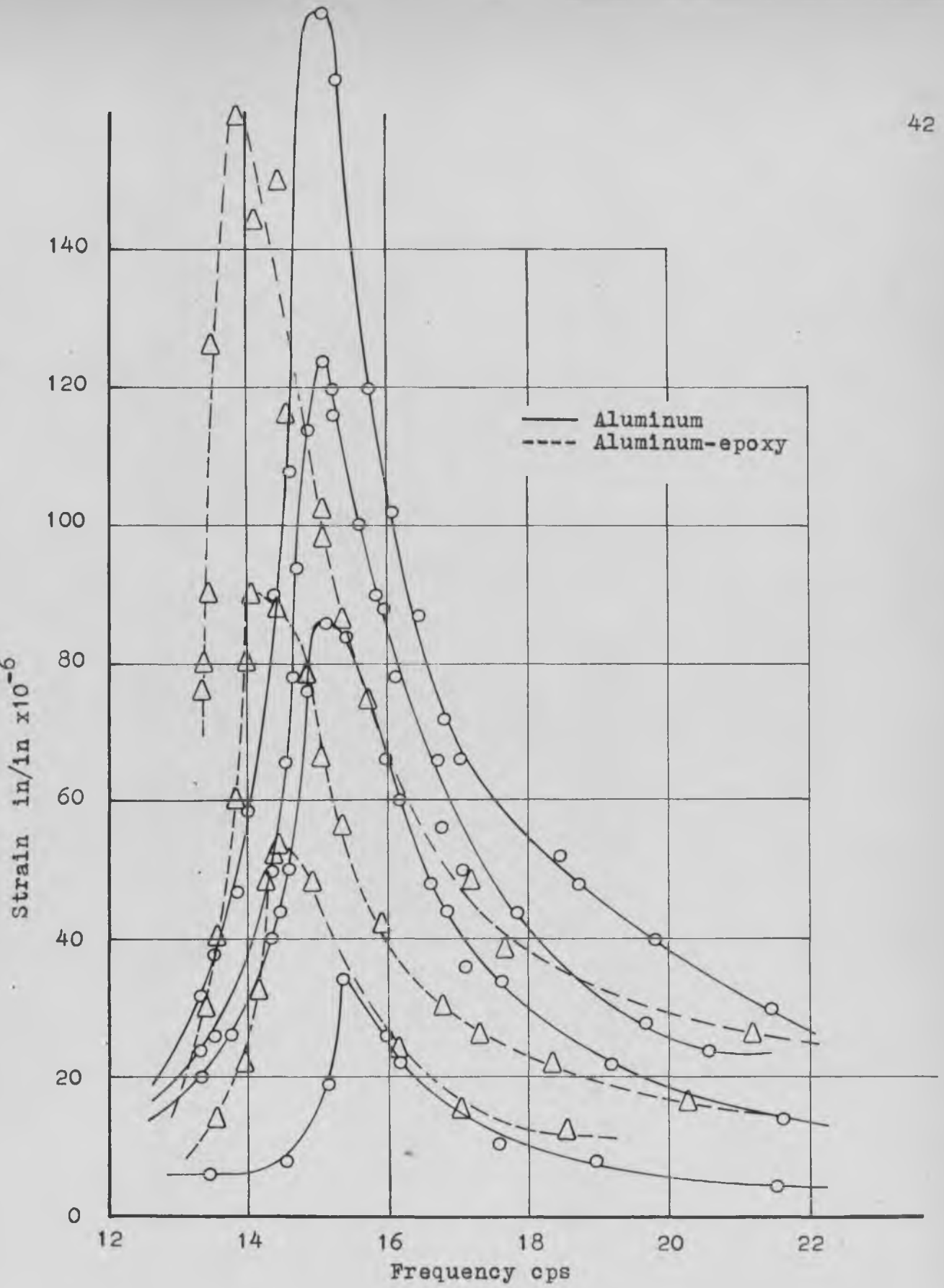

Figure 11
Forced response curve for aluminum model beam

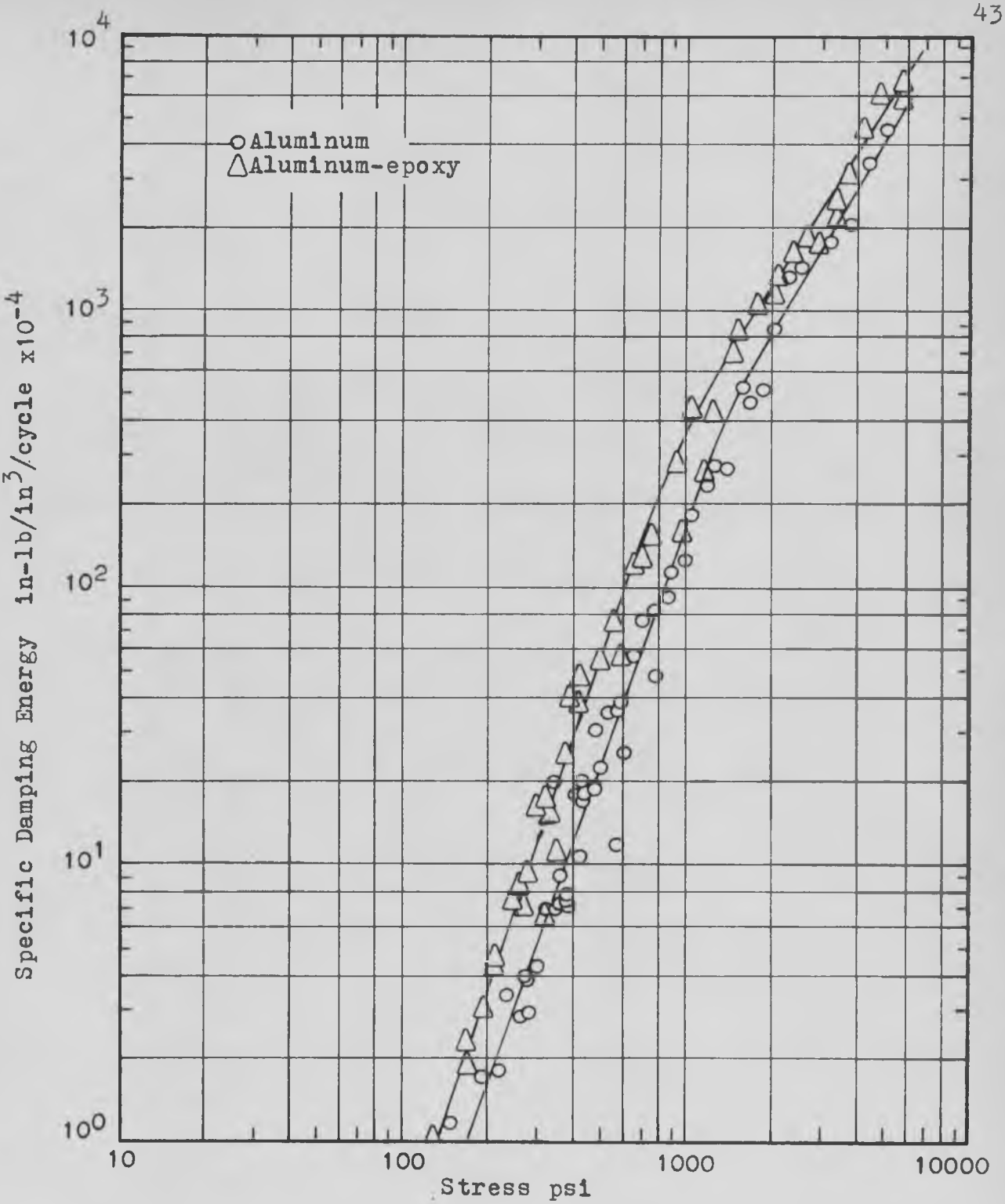

Figure 12
Specific damping energy as a function of strain
Model aluminum beam

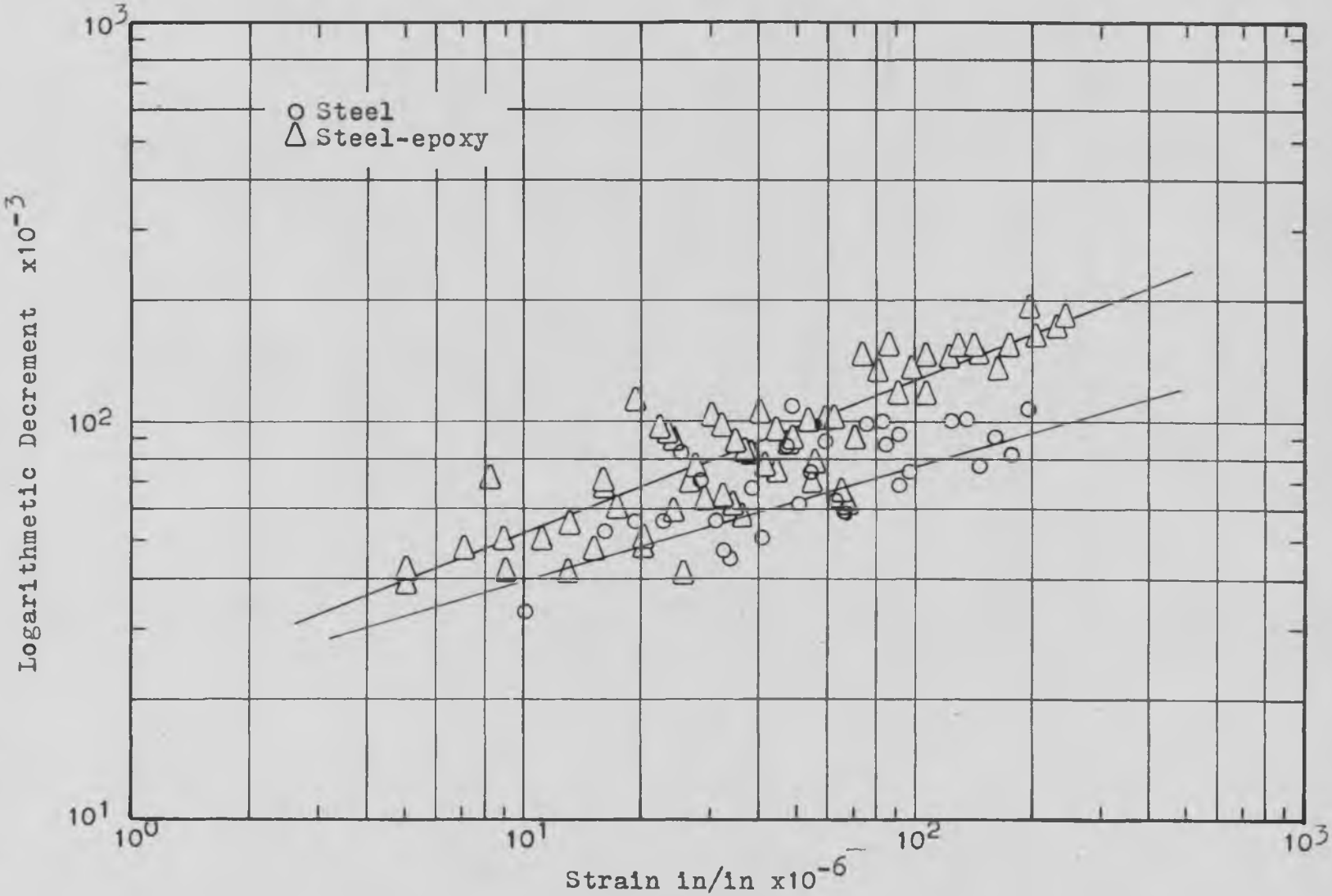

Figure 13
Logarithmic decrement vs strain plot for model steel beam

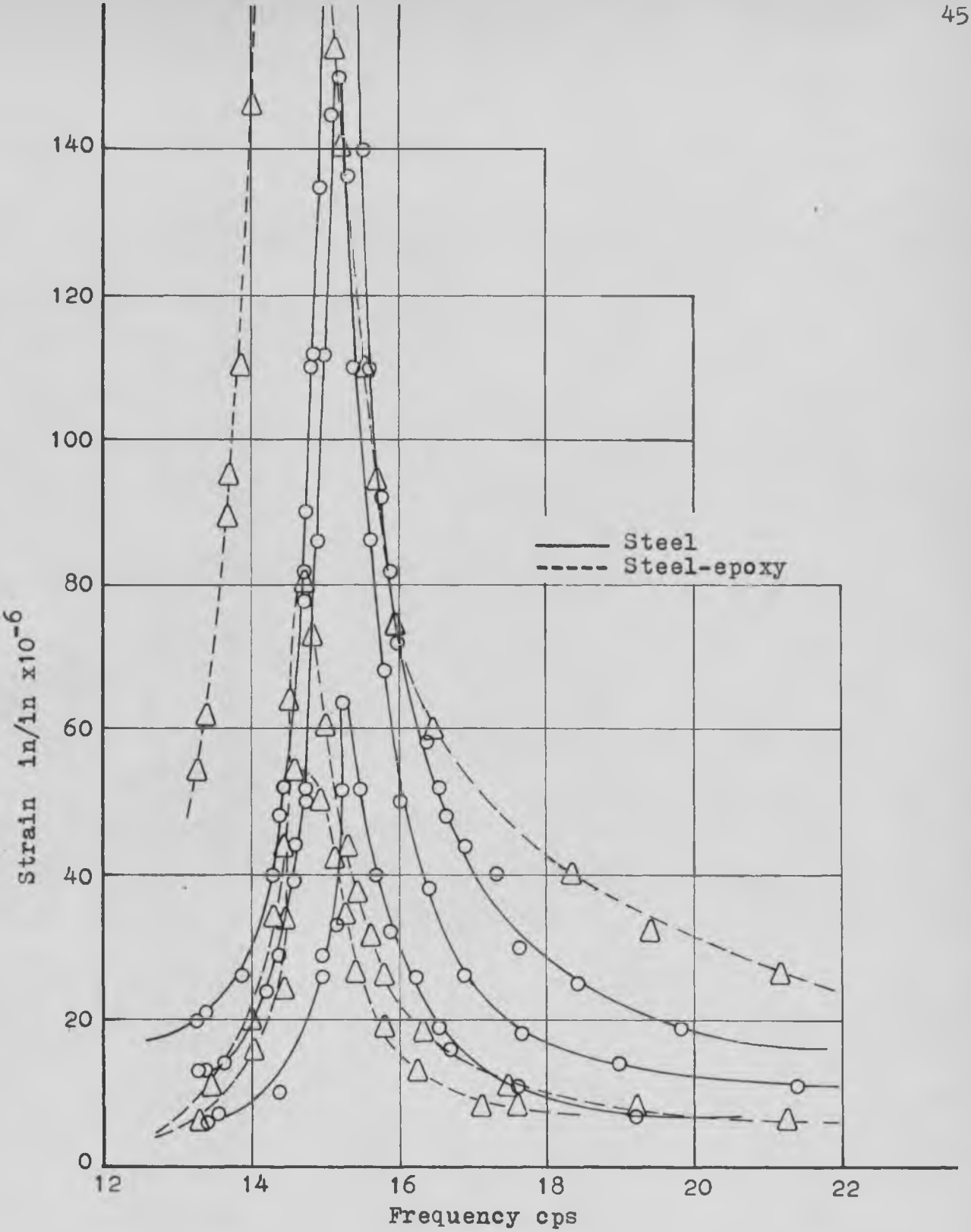

Figure 14
Forced response curve for steel model beam

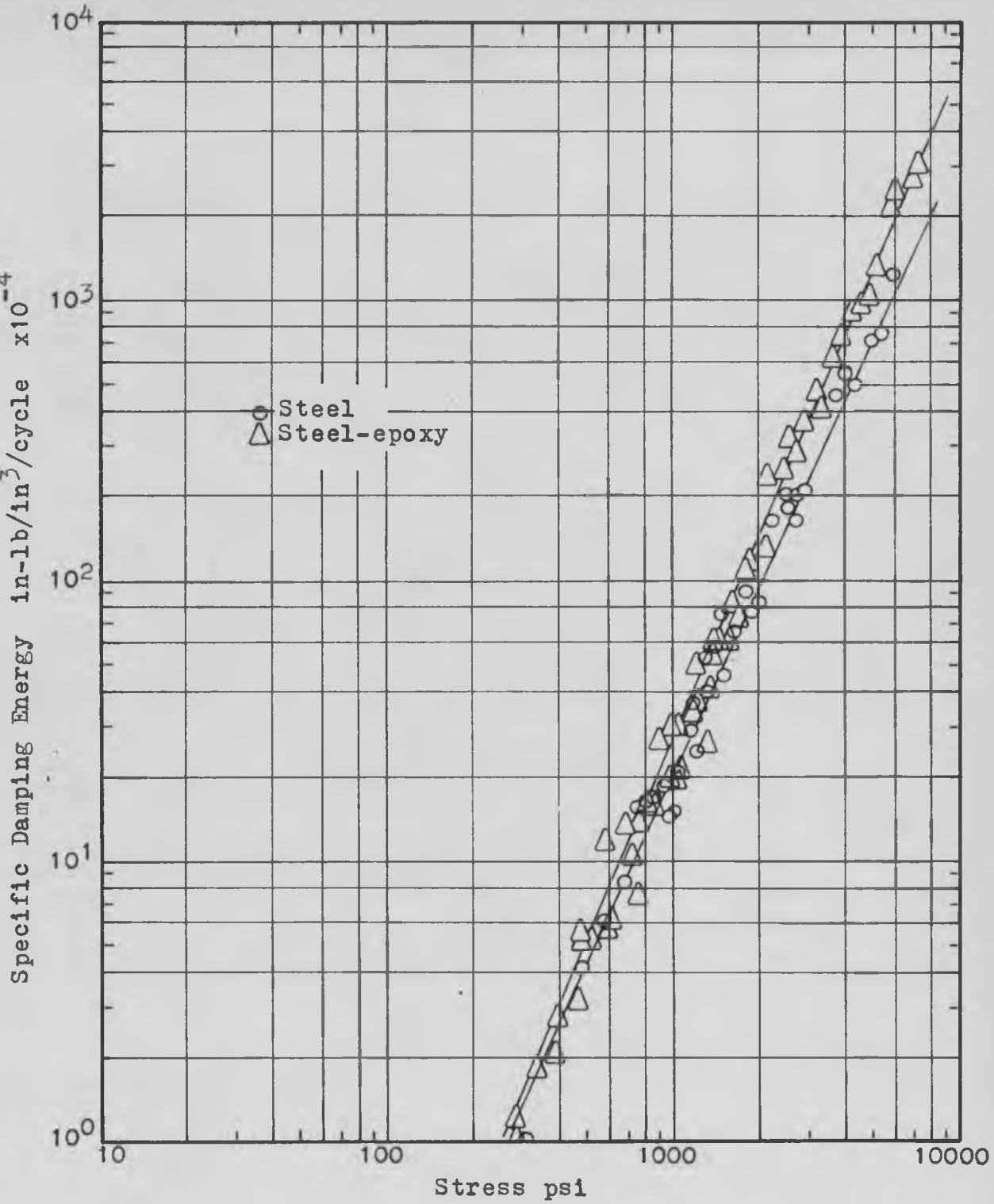

Figure 15
Specific damping energy as a function of strain
Model Steel Beam

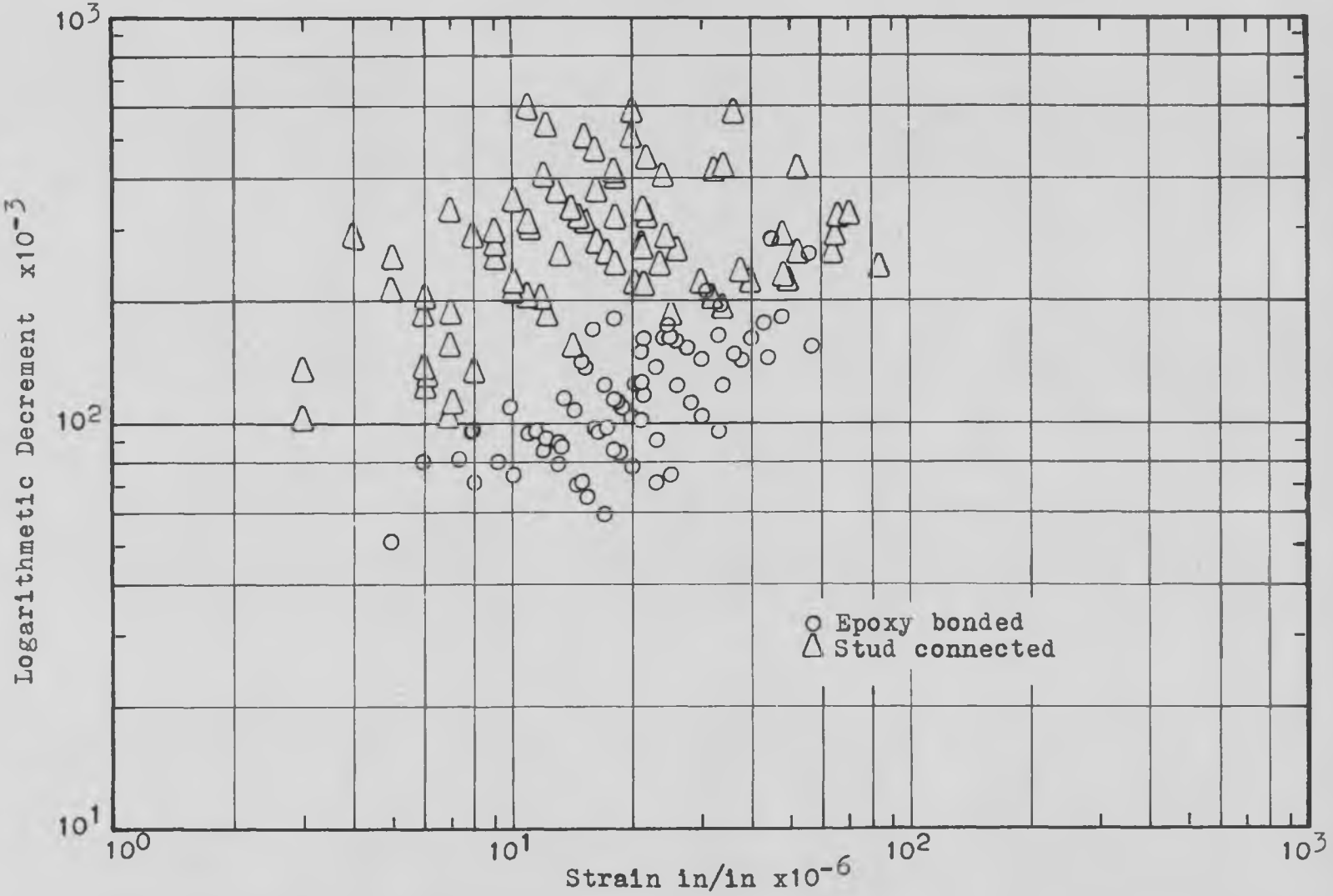

Figure 16
Logarithmic decrement vs strain plot for steel-concrete beams

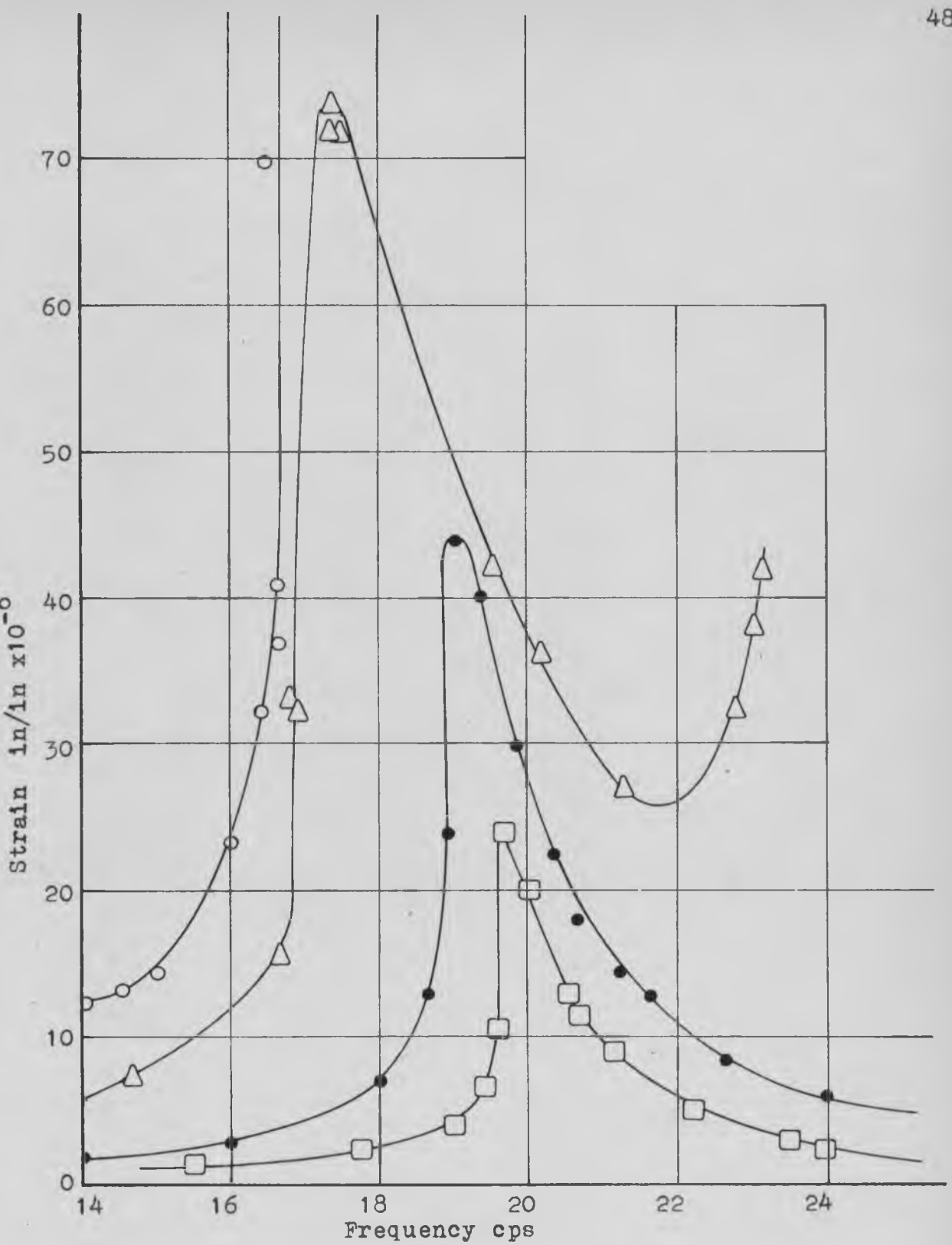

Figure 17
Forced response curve for steel-concrete beam; epoxy bonded

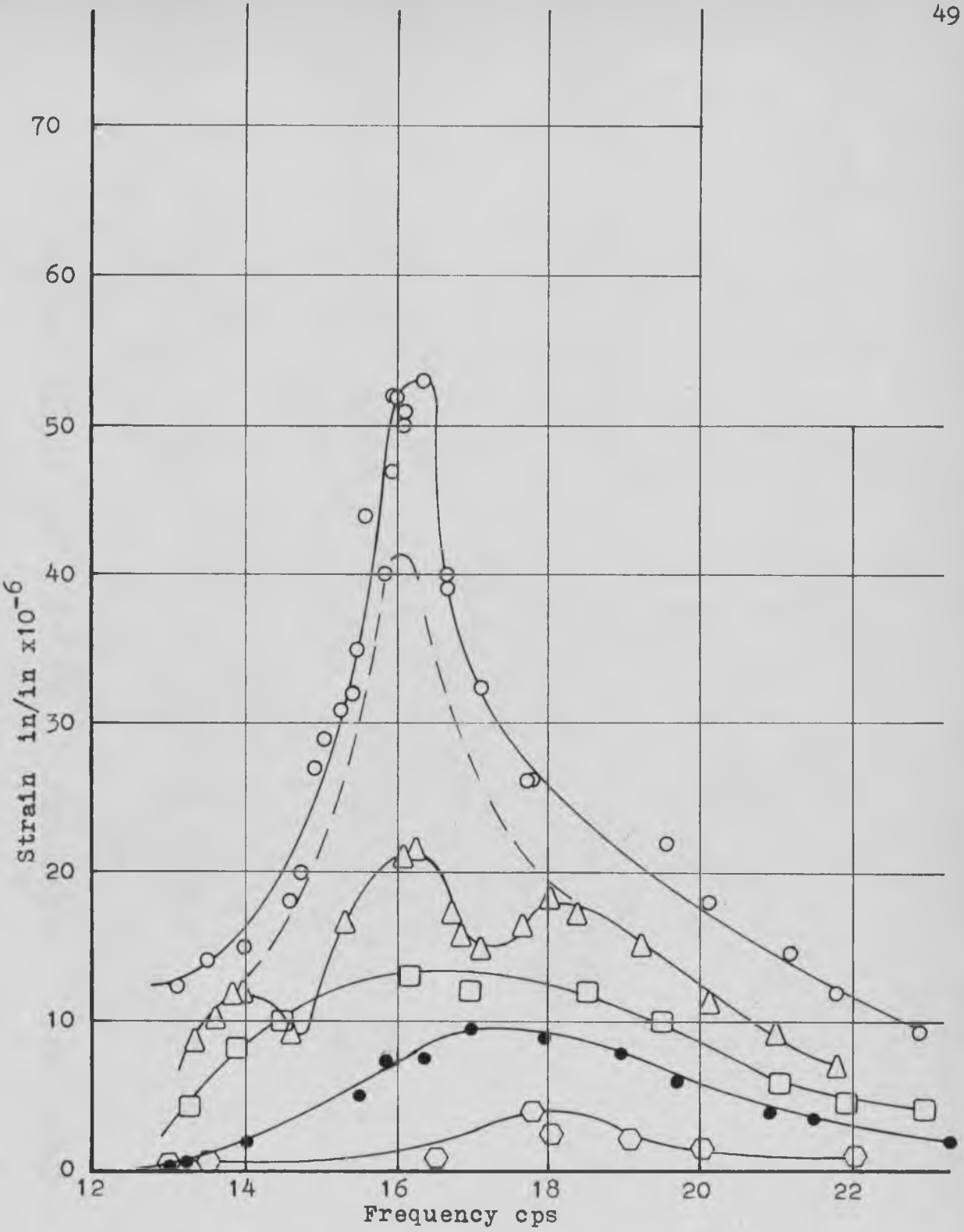

Figure 18
Forced response curve for steel-concrete beam; stud connected

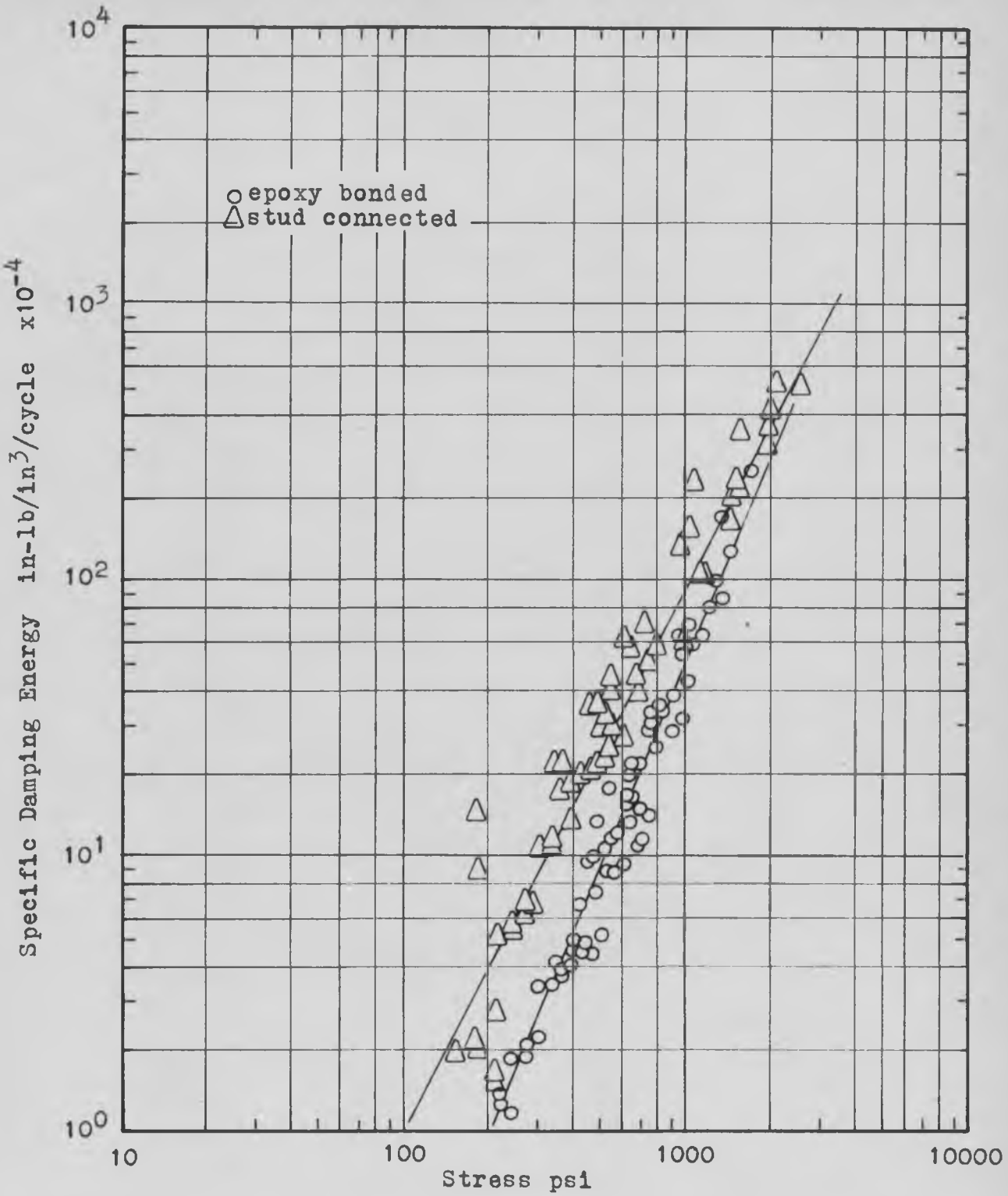

Figure 19
Specific damping energy as a function of strain
Composite Steel-concrete Beam

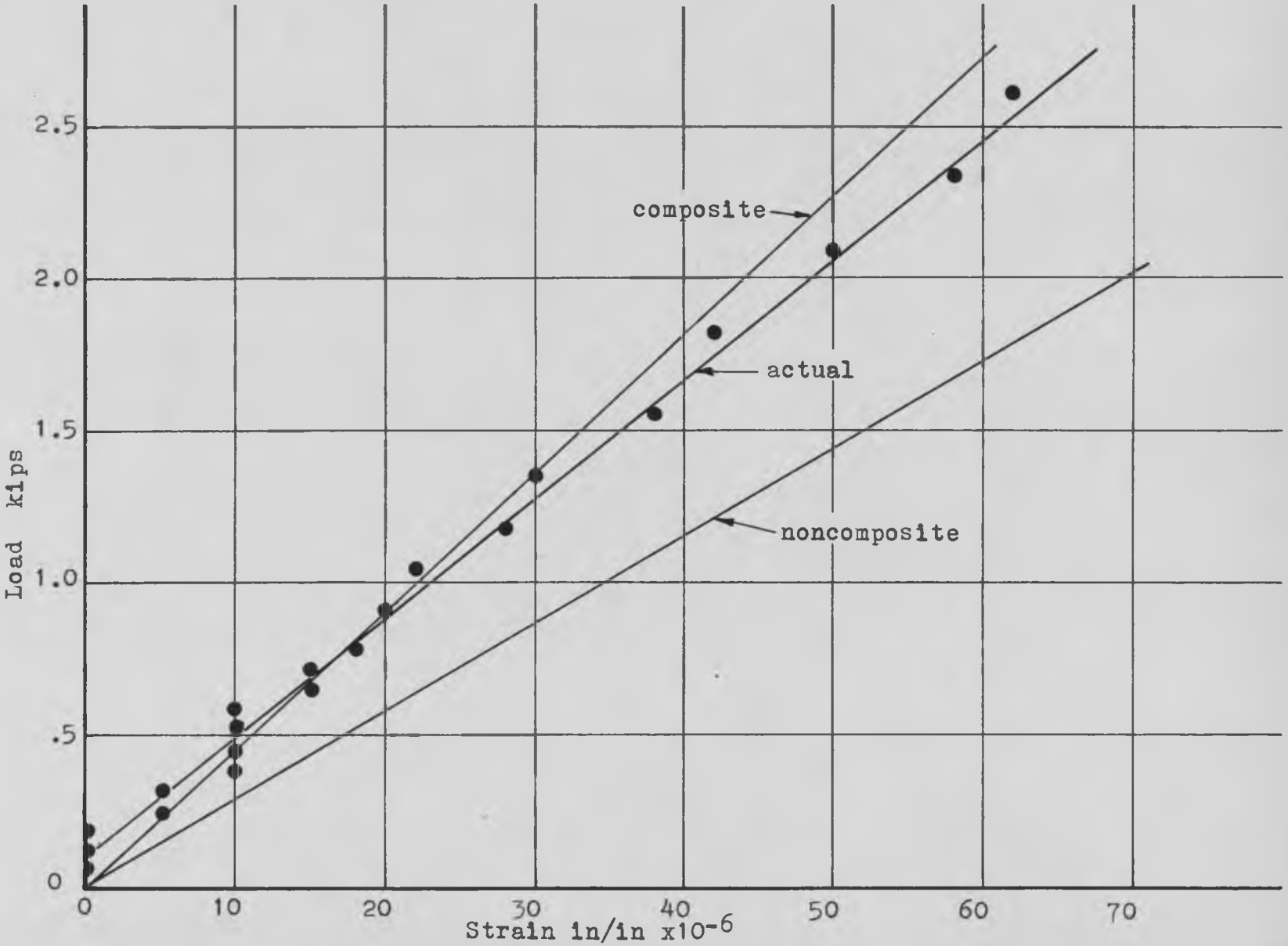

Figure 20
Load-strain curve for stud connected beam

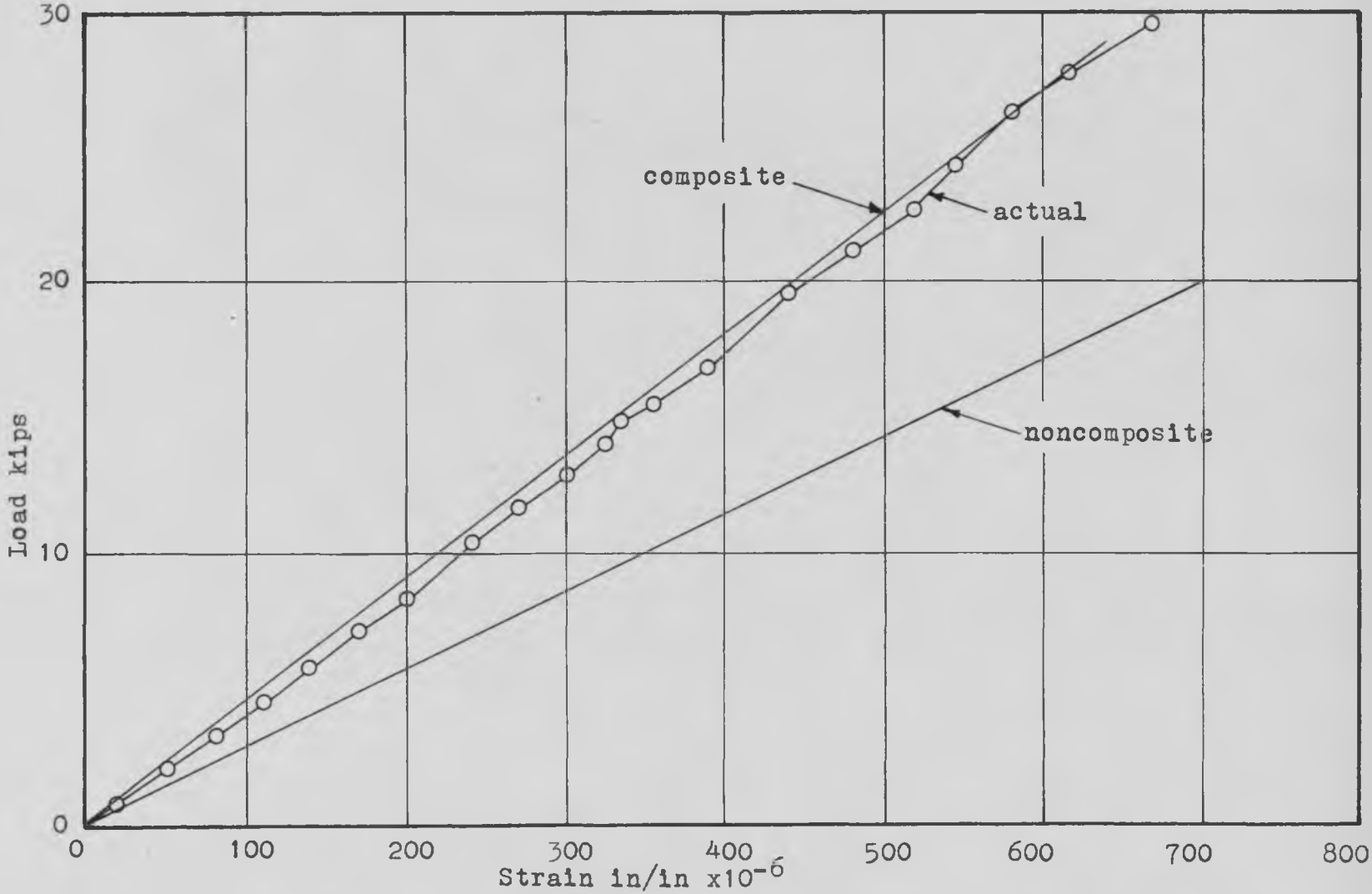

Figure 21
Load-strain curve for stud connected beam

Results

TABLE II
Natural Frequency cps

Beam	Theoretical	Experimental
Aluminum	15.3	15.1
Aluminum with epoxy	13.9	13.8
Steel	14.9	15.1
Steel	14.2	14.5
with epoxy	[illegible]	[illegible]
Steel-concrete epoxy bonded	26.8	17.3
Steel-concrete stud connected	26.8	16.3
Steel-concrete noncomposite	16.1	

TABLE III
Damping values for $c/(m_d)$ determined by the decay and forced response method.

Beam	Strain	Log-dec	Forced response
Aluminum	175	.0828	.0733
"	134	.0573	.0800
"	86	.0453	.0933
"	34	.0207	.0522
Aluminum epoxy	160	.1800	.1015
"	90	.1130	.0922
"	54	.0748	.0764
Steel	252	.0382	.0267
"	150	.0325	.0267
"	264	.0245	.0196
Steel epoxy	260	.0637	.0552
"	80	.0344	.0374
"	56	.0245	.0479
Steel-concrete epoxy bonded	74	.0748	.0863
"	42	.0622	.0395
"	24	.0414	.0279

TABLE IV
Experimental exponent values of (n)

Beam	n
Aluminum	2.85
Aluminum-epoxy	3.05
Steel	2.20
Steel-epoxy	2.37
Steel-concrete	
epoxy bonded	2.50
stud connected	2.00

Conclusions and Recommendations

The damping forces in the low stress region of an elastic material are found, from the testing of the model beams, to be dependent upon the amplitude of vibration. Also, the addition of a viscoelastic material to this system does not change the mechanism of damping, only the magnitude of the damping changes. The experimental natural frequencies of the model beams agree closely with the theoretical natural frequencies, and the reduced stiffness to mass ratio caused by the added epoxy has considerable effect on the natural frequency of the system. The addition of a viscoelastic material increases considerably the dissipated energy in lightly damped systems.

Results from the prototype beams are not all conclusive as was initially anticipated. A true knowledge of the action of these beams is not known because of their load history and the corresponding relationship between the concrete and steel. The cracks in the composite concrete slabs resulted in a large variation in the type of composite action that occurred. Results show that the concrete was not acting compositely and the steel was functioning alone. Experimental values show that the beams responded at the natural frequency for the noncomposite steel beam and not at the natural frequency of the composite steel-concrete beam. A linear damping theory should be used with caution for the prototype beam. The incomplete composite action of

these beams gave a very large spread in the ( ) values. It can be concluded that slippage friction is by far greater than the shear damping movement in the low stress region as is shown by comparing the results of the stud connected beam with the shear epoxy connected beam.

A study of the shear damping mechanism of the confined epoxy bonding material should be continued. Also, further studies in the stiffness effects of different connectors should be investigated.

As a result of this investigation many questions arise which should be investigated such as; the degree of composite action occurring in the low and high stress regions; the effects of load history on the response of the different beams; the effects of the type of material, slippage effects, and the magnitude of support damping.

REFERENCES

1. Bishop, R. E. D., "The Treatment of Damping Forces in Vibration Damping", Journal of Royal Aeronautical Science, Vol 59, p738-742, November 1955.

2. Pian, T. H. H., Structural Damping, chapter 5, edited by Crandall, S. H., "Random Vibration", Technology Press Wiley, 1958.

3. Dederman, A. H., "Dynamic Test of Two Cantilever Type Deck Steel Girder Bridges", Nebraska Department of Roads-Bridge Design Section, Lincoln Nebraska, 1961.

4. Hulsbos, C. L., and Linger, D. A., "Dynamic Tests of a Three-Span Continuous I-Beam Highway Bridge", Highway Research Board Bulletin 279, Bridge Design Studies and Piling Test, p28-29, 1960.

5. Kimball, A. L., "Vibration Prevention in Engineering", John Wiley, New York, p116, 1932.

6. Kriegh, J. D., and Endebrock, E. G., "The Use of Epoxy Resins in Reinforced Concrete", Static Final Progress Report, January 1963; Dynamic Final Progress Report, August 1963, Arizona Transportation and Traffic Institute, The University of Arizona.

7. Lazan, B. J., "Damping Properties of Materials and Material Composites", Applied Mechanics Review, Vol 2 No 5, p81-87, February 1962.

8. Lazan, B. J., Energy Dissipation Mechanisms in Structures with Particular Reference to Material Damping, section I, "Structural Damping", ASME, 1959, Reference 12.

9. Plunkett, P., Measurement of Damping, section V, "Structural Damping", ASME, 1959, Reference 12.

10. Robertson, J. M., and Yorgiadis, A. J., "Internal Friction of Engineering Materials", Journal of Applied Mechanics, Vol 13, 1946.

11. Ross, D., Ungar, E. E., and Kerwin Jr., E. M., Damping of Plate Flexual Vibrations by Means of Viscoelastic Laminae, section III, "Structural Damping", ASME, 1959, Reference 12.

12. Ruzicka, J. E., "Structural Damping", Shock and Vibration Committee of The Applied Mechanics Division of ASME, 1959.

13. Timoshenko, S., "Vibration Problems in Engineering", D. Van Nostrand Company, Inc., 3rd edition, 1955.

14. Tong, K. N., "Theory of Mechanical Vibration", John Wiley & Son, Inc., p82-89, 1960.

15. Zener, C., "Elasticity and Anelasticity", University of Chicago Press, 1948.

APPENDIX

TABLE 1A
DECAY RATE DATA - ALUMINUM BEAM

Strain	Stress	Logarithmic decrement	Spec.damp. energy	Strain	Stress	Logarithmic decrement	Spec.damp. energy
10.8	114	.02731	.000034	50	330	.08338	.002030
12.8	136	.02614	.000046	54	572	.11778	.003640
14	148	.05607	.000116	54	572	.03774	.001166
14.8	156	.03630	.000084	56	594	.11334	.003760
16.8	178	.03169	.000094	58	614	.07145	.002540
18	190	.05026	.000172	62	658	.13816	.005640
20.6	218	.04098	.000184	66	700	.16431	.007600
22	234	.06689	.000340	72	764	.14953	.008240
24.6	260	.04437	.000284	72	764	.08701	.004790
26	276	.05535	.000396	72	764	.08701	.004790
26	276	.05395	.000386	82	870	.13006	.009280
26	276	.05572	.000400	84	890	.15415	.011540
27	286	.03774	.000292	84	890	.15415	.011540
28.4	302	.05056	.000434	94	996	.13658	.012780
30	318	.07155	.000680	100	1060	.17435	.018480
31.2	330	.06626	.000682	100	1060	.17435	.018480
32	340	.06454	.000700	112	1188	.17521	.023320
34	360	.06063	.000740	120	1272	.18233	.027800
34.8	368	.07146	.000914	130	1378	.14905	.026700
36	382	.05716	.000780	150	1590	.22314	.053200
36	382	.05424	.000746	156	1654	.18233	.047000
37.2	394	.06670	.000706	176	1866	.15985	.052600
39.8	422	.06756	.001048	194	2056	.21801	.087200
40	424	.10536	.001800	226	2396	.25005	.135600
40	424	.10536	.001800	244	2586	.22931	.144800
41.4	438	.09628	.001746	296	3138	.19320	.179600
44	466	.09531	.001960	350	3710	.16758	.218000
44.2	480	.08783	.001930	426	4452	.18233	.341000
46	488	.13977	.003140	500	5300	.17435	.462000
48	508	.09258	.002260				

TABLE 1A
DECAY RATE DATA - ALUMINUM-EPOXY BEAM

Strain	Stress	Logarithmic decrement	Spec.damp. energy	Strain	Stress	Logarithmic decrement	Spec.damp. energy
8	85	.03836	.000026	47	498	.23923	.005600
8	85	.07192	.000050	50	530	.17028	.004500
10	106	.07438	.000078	52	552	.26237	.007540
12	128	.06758	.000104	53	562	.25671	.007600
12	128	.05792	.000090	62	658	.29850	.012180
16	170	.08219	.000224	66	700	.27764	.012840
16	170	.07192	.000196	70	742	.29726	.015440
18	190	.11956	.000410	88	932	.35021	.028700
20	212	.11157	.000472	92	976	.17331	.015560
20	212	.10536	.000448	100	1060	.41552	.044000
23	244	.13977	.000750	100	1060	.41552	.044000
25	264	.12783	.000844	112	1184	.19672	.026200
26	276	.13118	.000942	118	1250	.29335	.043200
26	276	.09710	.000696	140	1484	.33648	.069800
28	298	.19672	.001644	146	1548	.37844	.085600
30	318	.18233	.001740	168	1782	.35328	.105600
30	318	.14310	.001366	194	2056	.32623	.130200
30	318	.14310	.001360	200	2120	.31471	.133400
30	318	.06758	.000644	226	2396	.29657	.160600
32	340	.13353	.001454	254	2684	.26949	.184000
33	350	.09531	.001100	270	2862	.30011	.232000
36	382	.18233	.002500	280	2968	.21426	.178600
37	392	.14519	.002100	320	3392	.23099	.251000
40	424	.28768	.004880	346	3668	.24803	.315000
41	434	.21707	.003860	412	4368	.25271	.454000
46	488	.24513	.005500	456	4834	.27606	.610000
				550	5830	.28890	.694000
				546	5788	.18013	.570000

TABLE 1A
DECAY RATE DATA - Steel Beam

Strain	Stress	Logarithmic decrement	Spec.damp. energy	Strain	Stress	Logarithmic decrement	Spec.damp. energy
10	300	.03344	.000101	50	1500	.06188	.004640
16	480	.05374	.000412	54	1620	.07697	.006720
19	570	.05729	.000620	59	1770	.08856	.009240
22.5	674	.05636	.000854	63	1890	.06561	.007800
24.5	734	.08517	.001564	67	2010	.06157	.008320
26.5	794	.07848	.001652	74	2220	.09938	.016340
28.5	854	.07276	.001706	82	2460	.10266	.020700
30.5	914	.06783	.001890	90	2700	.09309	.020500
32	960	.04803	.001476	83	2490	.08823	.018240
33.5	1004	.04580	.001542	89	2670	.06980	.016580
35.5	1065	.05799	.002190	96	2880	.07574	.020900
38	1140	.06815	.002940	122	3660	.10354	.046200
39	1170	.08005	.003650	135	4050	.10126	.055400
40	1200	.05129	.002460	146	4380	.07834	.050200
43	1290	.09765	.005420	160	4800	.09144	.070200
43	1290	.07232	.004020	174	5220	.08388	.076200
47	1410	.08895	.005900	194	5820	.10881	.125200
48	1440	.11000	.007600				

TABLE 1A
DECAY RATE DATA - STEEL-EPOXY BEAM

Strain	Stress	Logarithmic decrement	Spec.damp. energy	Strain	Stress	Logarithmic decrement	Spec.damp. energy
5	150	.04264	.000032	38	1140	.08219	.003560
5	150	.03929	.000030	40	1200	.10536	.005060
7	210	.04807	.000070	41	1230	.07600	.003840
7	210	.04809	.000070	43	1290	.04764	.002640
9	270	.04188	.000102	44	1320	.09531	.005540
9	270	.05024	.000122	44	1320	.07367	.004280
11	330	.05017	.000182	46	1380	.09805	.006220
11	330	.05017	.000182	47	1410	.08895	.005900
13	390	.05569	.000282	48	1440	.09001	.006220
13	390	.04186	.000212	53	1590	.09909	.008360
15	450	.04770	.000322	54	1620	.06827	.005980
16	480	.06921	.000532	56	1680	.07870	.007420
16	480	.07320	.000560	60	1800	.10536	.011380
17	510	.06063	.000526	62	1860	.10179	.011720
19	570	.11124	.001204	64	1920	.06454	.008920
20	600	.05129	.000616	70	2100	.08962	.013180
20	600	.04795	.000576	72	2160	.14953	.023200
22	660	.09531	.001386	80	2400	.13353	.025600
24	720	.09116	.001576	84	2520	.15415	.032600
24	720	.08701	.001506	90	2700	.11778	.028600
24	720	.05990	.001040	96	2880	.13353	.036900
25	750	.04082	.000766	104	3120	.14459	.046800
26	780	.06936	.001400	108	3240	.11779	.041200
27	810	.07697	.001684	120	3600	.14310	.061800
29	870	.06308	.001594	126	3780	.15415	.073400
30	900	.10536	.002840	140	4200	.15415	.090600
32	960	.09844	.003020	146	4380	.14733	.094400
32	960	.06454	.001984	160	4800	.13353	.102600
34	1020	.06063	.001980	170	5100	.15220	.132200
34	1020	.06333	.002200	194	5820	.19269	.218000
35	1050	.08962	.001986	200	6000	.16252	.195000
36	1080	.05711	.002220	230	6900	.17023	.270000
36	1080	.08136	.003160	240	7200	.18233	.315000

TABLE 1A
DECAY RATE DATA - STEEL-CONCRETE, EPOXY BONDED

Strain	Stress	Logarithmic decrement	Spec.damp. energy	Strain	Stress	Logarithmic decrement	Spec.damp. energy
6	180	.08109	.000117	18.5	554	.08457	.000866
6	180	.05109	.000082	19	570	.11123	.001202
7.2	216	.08138	.000126	20	600	.07796	.000934
8	240	.09589	.000184	20	600	.10536	.001264
8	240	.07192	.000138	20.4	612	.12517	.001564
9	270	.08397	.000188	21	630	.14860	.001968
9.2	276	.08171	.000207	21	630	.12675	.001676
10	300	.11157	.000334	21	630	.10009	.001326
10	300	.07438	.000223	21.2	636	.16364	.002210
11.4	342	.10721	.000418	21.6	648	.11778	.001646
11	330	.09531	.000346	22.4	674	.06900	.001048
12	360	.08702	.000376	23	690	.13977	.002220
12	360	.09116	.000394	23	690	.09088	.001440
13	390	.08005	.000406	23.2	696	.07146	.001154
13	390	.08005	.000406	24	720	.16252	.002800
13	390	.09194	.000466	25	750	.16487	.003090
13.5	408	.08823	.000490	25	750	.17435	.008700
14.5	434	.10920	.000686	25	750	.07472	.001400
14.5	434	.07146	.000450	26	780	.12261	.002480
15	450	.14310	.000966	27	810	.16034	.002220
15	450	.07155	.000482	28	840	.15415	.003630
15	450	.14310	.000966	30	900	.14310	.003860
15.5	465	.06670	.000450	30	900	.10536	.003500
15.6	468	.13721	.001002	31	930	.21511	.006200
16	480	.17329	.001330	33	990	.09531	.003110
16	480	.09844	.000756	33	990	.16430	.005360
17	510	.06063	.000526	34	1020	.19417	.006740
17	510	.09875	.000876	34	1020	.12517	.004340
17	510	.12515	.001084	36	1080	.14953	.005820
18	540	.11778	.001146	38	1140	.14108	.006120
18	540.	.08701	.000846	40	1200	.16252	.007800
18	540	.18233	.001774	43	1290	.17769	.009860
18.5	554	.11441	.001174	44	1320	.14661	.008500
19	570	.11000	.001216	48	1440	.18233	.001260
				56	1680	.26416	.024900

TABLE 1A

DECAY RATE DATA - STEEL-CONCRETE BEAM, STUD CONNECTED

Strain	Stress	Logarithmic decrement	Spec.damp. energy	Strain	Stress	Logarithmic decrement	Spec.damp. energy
3	90	.10136	.000028	16	480	.37469	.002880
3	90	.13849	.000036	16	480	.47000	.003610
5	150	.25542	.000192	16	480	.28768	.002200
6	180	.13515	.000146	16	480	.28768	.002200
6	180	.08109	.000088	17	510	.26827	.002330
6	180	.20273	.000218	18	540	.40546	.003940
6	180	.18233	.000198	18	540	.32543	.003160
7	210	.18654	.000274	18	540	.25131	.002440
7	210	.15415	.000226	18	540	.40546	.003940
7	210	.11216	.000165	20	600	.51083	.006120
7	210	.10280	.000152	20	600	.22314	.002680
7	210	.33648	.000494	20	600	.22314	.002680
8	240	.28768	.000552	21	630	.33648	.004460
8	240	.28768	.000560	22	660	.46199	.006560
8	240	.28768	.000552	24	720	.45046	.007000
9	270	.25133	.000610	23	90	.24513	.003890
9	270	.27033	.000658	24	720	.28768	.004960
10	300	.35667	.001070	26	780	.26237	.005320
10	300	.22314	.000670	30	900	.22314	.006020
10	300	.22314	.000670	30	900	.22314	.006020
10	300	.35667	.001070	32	960	.42121	.012940
10	300	.22314	.000670	34	1020	.43533	.015100
11	330	.30307	.001100	34	1020	.19417	.006740
11	330	.60614	.002200	36	1080	.58780	.022800
11	330	.31846	.001156	38	1140	.23639	.010260
11	330	.31846	.001156	40	1200	.22314	.010720
12	360	.40546	.001752	48	1440	.23362	.016140
12	360	.40546	.001752	48	1440	.28768	.019860
12	360	.53900	.002230	50	1500	.22314	.016740
13	390	.26237	.001332	52	1560	.42489	.034400
13	390	.36774	.001860	52	1560	.26237	.021300
14	420	.33648	.001980	64	1920	.24686	.030300
15	450	.51053	.003550	64	1920	.28768	.035300
15	450	.31016	.002090	66	1980	.31846	.041600
15	450	.31016	.002090	72	2160	.32543	.050600
				84	2520	.24117	.051000

TABLE 2A
FORCE RESPONSE DATA

BEAM	RUN	STRAIN	FREQUENCY
Aluminum	1	6	13.6
		8	14.6
		19	15.1
		34	15.3
		26	15.94
		22	16.1
		10	17.3
		8	18.8
		4	21.6
	2	20	13.3
		20	13.5
		26	13.75
		40	14.3
		44	14.5
		50	14.6
		76	14.8
		86	15.1
		84	15.4
		66	15.9
		60	16.1
		48	16.5
		44	16.8
		36	17.0
		34	17.6
		30	18.5
		22	19.1
		14	21.6
	3	24	13.3
		26	13.5
		50	14.3
		66	14.5
		78	14.6
		94	14.65
		114	14.8
		124	15.0
		120	15.15
		116	15.15
		100	15.6
		90	15.8
		88	15.9
		78	16.1
		66	16.7
		56	16.7
		50	17.0
		44	17.8
		28	19.6
		24	20.5
Aluminum	4	32	13.3
		38	13.5
		47	13.8
		59	14.0
		90	14.3
		108	14.5
		175	15.00
		165	15.15
		120	15.7
		102	16.0
		87	16.75
		66	16.95
		52	18.42
		48	18.65
		40	19.75
		30	21.4
		20	23.5
Aluminum epoxy	1	12	13.4
		14	13.5
		22	14.0
		52	14.3
		48	14.2
		54	14.4
		48	14.9
		32	14.1
		22	13.9
		24	16.1
		15	17.0
		12	18.5
		8	22.5
	2	30	13.35
		40	13.5
		60	13.8
		80	13.95
		90	14.05
		88	14.4
		78	14.8
		66	15.0
		56	15.3
		42	15.9
		30	16.7
		26	17.3
		22	18.3
		16	20.2

TABLE 2A
FORCE RESPONSE DATA

BEAM	RUN	STRAIN	FREQUENCY
Aluminum epoxy	3	76	13.3
		80	13.5
		90	13.4
		126	13.45
		160	13.8
		160	13.75
		144	14.0
		150	14.4
		116	14.5
		98	15.0
		102	15.0
		83	15.3
		74	15.7
		64	16.1
		40	17.15
		48	17.15
		38	18.6
		26	21.1
		22	24.7
Steel	1	6	13.4
		7	13.55
		10	14.4
		26	15.0
		29	15.0
		33	15.15
		52	15.25
		64	15.25
		52	15.5
		40	15.7
		32	15.9
		26	16.2
		19	16.6
		16.	16.7
		11	17.65
		7	19.2
	2	13	13.3
		13	13.4
		14	13.7
		24	14.2
		29	14.4
		39	14.6
		44	14.6
		50	14.75
		52	14.8
		86	14.9
Steel	2	90	14.75
		112	15.0
		145	15.1
		150	15.2
		136	15.3
		110	15.4
		86	15.6
		68	15.8
		50	16.05
		38	16.4
		26	16.9
		18	17.7
		14	19.0
		11	21.4
	3	20	13.3
		21	13.4
		26	13.9
		40	14.3
		48	14.4
		52	14.5
		78	14.8
		82	14.75
		110	14.85
		112	14.9
		135	15.0
		175	14.95
		200	15.05
		108	15.0
		122	15.1
		126	15.17
		120	15.2
		100	15.25
		92	15.4
		70	15.5
		55	15.6
		46	15.8
		41	15.9
		36	16.0
		29	16.4
		26	16.55
		24	16.7
		22	16.9
		20	17.35
		15	17.65
		12.5	18.5
		9.5	19.8
		8	21.6

TABLE 2A
FORCE RESPONSE DATA

BEAM	RUN	STRAIN	FREQUENCY
Steel-epoxy	1	8	13.3
		11	13.5
		16	14.1
		24	14.46
		34	14.46
		44	14.47
		54	14.58
		50	14.9
		45	15.1
		42	15.1
		34	15.2
		32	15.4
		26	15.4
		22	15.7
		19	15.8
		13	16.25
		8	17.1
		8	17.7
	2	10	13.4
		12	13.5
		14	13.8
		20	14.0
		34	14.3
		43	14.4
		45	14.45
		64	14.5
		74	14.75
		80	14.75
		73	14.86
		60	15.0
		44	15.3
		37	15.5
		31	15.6
		26	15.8
		18	16.3
		11	17.5
		8	19.2
		6	21.25
	3	12	13.05
		30	13.1
		54	13.24
		54	13.33
		62	13.43
		89	13.7
		95	13.69
		110	13.85
		146	13.98
		204	14.08
		240	14.14
Steel-epoxy	3	250	14.22
		260	14.45
		220	14.66
		210	14.71
		194	14.81
		184	14.89
		170	15.0
		154	15.07
		140	15.22
		110	15.49
		94	15.71
		74	15.94
		60	16.47
		40	18.33
		32	19.4
		26	21.18
Steel-concrete epoxy bonded	1	1.5	15.50
		2.5	17.75
		4	19.00
		65	19.39
		10.5	19.60
		24	19.67
		20	20.00
		13	20.57
		11.5	20.67
		9	21.13
		5	22.20
		3	23.50
		2.5	24.00
		1.5	26.00
	2	2	14.00
		3	16.00
		7	18.00
		13	18.67
		24	18.89
		44	19.00
		40	19.35
		30	18.86
		22.5	20.31
		18	20.67
		14.5	21.19
		13	21.67
		8.5	22.67
		6	24.00
		4.5	25.67
		4.0	28.50

TABLE 2A
FORCE RESPONSE DATA

BEAM	RUN	STRAIN	FREQUENCY
Steel-Concrete epoxy bonded	3	7.5	14.67
		15.5	16.67
		32	16.92
		33	16.84
		74	17.33
		72	17.33
		72	17.50
		42	19.54
		36	20.14
		27	21.25
		32	22.79
		38	23.03
		42	23.16
	4	12.5	14.00
		13.5	14.50
		14.5	15.00
		23.5	16.00
		32.5	16.40
		70	16.43
		37	16.67
		41	16.67
		98	16.67
Steel-concrete stud connected	1	.5	13.0
		.6	13.5
		1	16.5
		4	17.78
		2.2	18.00
		2.2	19.05
		1.4	20.00
		1	22.00
		1.6	25.401
	2	.6	13.20
		2	14.00
		5	15.50
		7.5	15.88
		7.5	16.36
		9.5	16.95
		9	17.93
		8	18.95
		6	19.66
		4	20.61
		3.5	21.51
		2	23.33
	3	4.5	13.30
		8	13.90
		4	13.90
		9	13.96
Steel-concrete stud connected	3	10	15.48
		13	16.09
		12	16.99
		13	18.50
		10	19.29
		6	20.93
		5.6	21.08
		4.4	21.92
		4	23.03
		4	24.44
		13	16.25
	4	8.5	13.30
		10	13.43
		12	13.83
		12	13.96
		9	14.61
		16.5	15.29
		21	16.07
		21.5	16.22
		17	16.67
		15.5	16.86
		15	17.09
		16.5	17.65
		18	18.00
		17	18.36
		15	19.19
		11.2	20.11
		9	20.95
		7	21.82
	5	12.5	13.10
		14.2	13.50
		15	14.00
		20	14.75
		29	15.05
		31	15.19
		32	15.45
		40	15.87
		50	16.13
		53	16.36
		52	16.02
		51	16.13
		47	15.95
		35	15.44
		31	15.28
		27	14.94
		18	14.61
		44	15.56
		40	16.67

TABLE 2A
FORCE RESPONSE DATA

BEAM	RUN	STRAIN	FREQUENCY
Steel-concrete stud connected	5	32.6	17.11
		26.2	17.70
		26.2	17.81
		22	19.57
		18	20.12
		14.8	21.18
		12	21.79
		9.2	22.89

TABLE 3A
LOAD-STRAIN FOR STUD CONNECTED BEAM

LOAD	STRAIN	STRESS	LOAD	STRAIN	STRESS	LOAD	STRAIN	STRESS
65	0	0	1175	28	840	10448	240	7200
130	0	0	1360	30	900	11754	270	8100
196	0	0	1567	38	1140	13060	300	9000
261	5	150	1828	42	1260	14366	325	9750
327	5	150	2090	50	1500	15019	340	10200
392	10	300	2351	58	1740	15672	355	10650
457	10	300	2612	62	1860	16978	390	11700
522	10	300	2873	68	2040	19590	440	13200
588	10	300	3134	75	2250	21225	480	14400
653	15	450	3657	88	2640	22855	510	15300
718	15	450	4898	115	3450	24488	545	16350
784	18	540	5877	139	4170	26120	580	17400
914	20	600	7183	170	5100	27752	615	18450
1045	22	660	8489	200	6000	29385	670	20100